Supporting Information

Design, Synthesis, and Evaluation of Bifunctional Acridine-Naphthalenediimide Redox-Active Conjugates as Antimalarials

Srikanta Dana,[†,§] *Sudhir Kumar Keshri*,[†] *Jyoti Shukla*,[†] *Kunwar Somesh Vikramdeo*,[‡] *Neelima Mondal*,[‡] *Pritam Mukhopadhyay*,[*,†,] *and Suman Kumar Dhar*,[*,§]

[†]Jawaharlal Nehru University, Supramolecular and Material Chemistry Lab, School of Physical Sciences, New Mehrauli Road, 110067, New Delhi, India.

[‡]Jawaharlal Nehru University, School of Life Sciences, New Mehrauli Road, 110067, New Delhi, India.

[§]Jawaharlal Nehru University, Special Centre for Molecular Medicine, Jawaharlal Nehru University, New Mehrauli Road, 110067, New Delhi, India.

Table of contents **Pages**

Experimental Section

Cytotoxicity assay: Cell viability in response to drugs was evaluated by using MTT assay.[1] NIH3T3 cells (4000cells/well) were plated in 200 µl DMEM in 96-well plate (flat bottom) in the presence of various concentrations of the tested compounds along with only DMSO (control) for different length of time (24 h and 48 h) in a humidified CO_2 incubator at 37 ºC. At the end of the stipulated time interval, 20 µl of MTT (5 mg/ml in PBS) solution was added to each well and incubated for 4 h in the CO_2 incubator. After 4 h, medium along with the MTT solution of plates were discarded carefully followed by addition of DMSO (200ul) in each well. Formazan crystals were dissolved by further incubating the plates for additional 1 hour in CO_2. After 1 h, absorbance was taken in ELISA microplate reader at 570 nm wavelength. The percentage of cell viability was calculated by following equation.

$$\text{cell viability} = \frac{\text{Abs}_{570\ \text{nm}}\ \text{of the test sample}}{\text{Abs}_{570\ \text{nm}}\ \text{of the control}} \times 100\ \%$$

Heme binding studies: Stock solution of heme [FPIX(Fe^{+3})Cl] (1.2 mM) and drug (molecule 1a, 2.5 mM) were prepared in cell culture grade DMSO. A 2.4 µM working solution of heme was prepared by addition of 20 µl of heme stock (1.2 mM) solution into a mixture of 4 mL UV grade DMSO and 1ml 0.2 M HEPES buffer (pH 7.4) and then the volume of the solution was adjusted to 10 mL by double distilled deionized water. The titration experiment was performed in a 3 ml quartz cuvette varying the concentration of drug (0-4.52 µM) and keeping the heme concentration constant (2.4 µM). Following each addition, sample was mixed and equilibrated for 5 min and UV-visible spectra were recorded on a JASCO, V-670 model spectrophotometer. The binding constant was evaluated by fitting the absorbance data in a 1:1 binding model using nonlinear regression analysis method in Graphpad Prism 6 software.

DNA binding studies: Calf thymus (CT) DNA [λmax (ε) = 260 nm (6600 $M^{-1}cm^{-1}$)] pellet was dissolved in TE buffer (10 mM Tris-Cl, 1 mM EDTA, pH 8) to prepare stock solution. Drug (0.06 mM) was titrated with increasing concentrations of CT DNA (0-0.70 mM) in 1:3 TE buffer/MeOH and UV-visible spectra were recorded in a same manner as mentioned above. The absorbance of the each samples were plotted against wavelengths using Origin 8.5 pro software to generate the titration plots.

JC-1 assay for measuring mitochondrial membrane potential: Mitochondrial membrane potential ($\Delta\Psi_m$) was investigated using JC-1 (Molecular Probes, Invitrogen) dye following an adaptation of the protocols previously reported elsewhere.[2] JC-1, 5,5',6,6'-tetrachloro-1,1',3,3'-tetarethylbenzimidazolocarbocyanine iodide, is a cell permeable membrane potential sensitive cationic dye. It emits green fluorescence (emission 525 nm) in its monomeric form. Upon transfer to the polarized mitochondria (functionally active) it forms J-aggregates and emits aggregation dependent red-orange fluorescence (emission 590 nm). Depolarized mitochondria (functionally in active) exhibits monomer with green fluorescence. Thus, it is possible to discriminate $\Delta\Psi_m$ by fluorescence microscope equipped with standard fluorescein long-pass optical filter using JC-1 dye. Briefly, synchronized ring stage (~ 12 h post invasion) parasites were grown in presence or absence of different concentrations of drug to complete one life cycle. Parasite cultures were aliquoted at different time points and then washed with room temperature PBS followed by incubation with JC-1 for 30 mins at 37 ºC. After JC-1 incubation, parasites were washed with room temperature PBS and subsequently the wet mount slides were observed under fluorescence microscope (ZIEES) using FITC (for monomer) and rhodamine (for J-aggregates) filters.

Cyclic voltammetry (CV) and Differential pulse voltammetry (DPV): CV and DPV was carried out using a computer controlled potentiostat (CHI 650C) and a standard three electrode arrangement that consisted of platinum working and auxiliary electrodes and saturated calomel (SCE) as reference electrode. The electrochemical measurements were carried out in argon-purged solvents containingn-Bu_4NPF_6 (0.1 M) as supporting electrolyte. The scan rates for CV experiments were typically 200-300 mV/s. DPV was carried out keeping peak amplitude 50 mV, peak width 0.01 sec, pulse period 0.05 sec and increment E at 20 mV.

Theoretical Calculations: All theoretical calculations were done using the Gaussian 09 quantum chemistry program package. Density function calculations (DFT) at the B3LYP/6311^{++}G(d,p) level were used to investigate the ground state optimized structure. The frontier molecular orbitals and electrostatic potentials (ESP) mapped on the electronic density surfaces are based on the DFT calculations and plotted in the GaussView 5.0 program.

X-ray Crystallography: Crystals of **1b** were grown in DMSO solution by slow evaporation method at 25ºC. The crystals were adequately stable under ambient conditions, losing the crystalline nature for long exposure to air. The reported data set was collected by mounting the crystal with paratone oil in a loop. X-ray reflections were collected on Bruker D8 Questdiffractometer with CMOS detector using Mo-Kα radiation, generated from the micro-focus sealed tube. Data collection was performed using φ and ω-scans of 0.5° steps at 100 K. Cell determination, data collection and data reduction were performed with the help of Bruker APEX2 (version: 2014.3-0) software. The structure were solved by intrinsic phasing method (SHELXS-97) and refined by full-matrix least squares refinement method based on F^2, using, SHELXL-2014. A total of 48923 reflections were measured out of which 6948 were independent and 4608 were observed [I > 2\s(I)] for theta 28.37°. All non-hydrogen atoms were refined anisotropically. All hydrogen atoms were fixed geometrically with their U_{iso} values 1.2 times of the phenylene and methylene carbons and 1.5 times of the methyl carbon using a riding model. The refinement showed a highly disordered dimethylsulphoxide molecule, which could not be modelled satisfactorily. Therefore it was removed by using SQUEEZE routine of PLATON. A final refinement of 392 parameters has given R1 = 0.0702, wR2 = 0.1866 for the observed data. The ORTEP diagram is given in Figure S2 in this supporting information. The crystal structure data are deposited to Cambridge Structural Database with CCDC 1439860.

Table S1: Selected bond lengths and torsional angles of the crystal structure of **1b**.

Atoms	**Selected Bond length [Å]**	**Atoms**	**Selected Bond length [Å]**
C11−O3, C13−O1	1.208	N2−C13	1.405
C12−O4	1.216	C1−C11	1.478
C14−O2	1.216	C4−C12	1.474
N1−C11	1.399	C5−C13	1.479
N1−C15	1.476	C8−C14	1.479
N1−C14	1.395	C2−C3	1.395
N2−C19	1.446	C6−C7	1.394
N2−12	1.398	C9−C10	1.409
Atoms	**Selected Torsion Angles [°]**		**Selected Torsion Angles [°]**
C12−N2−C19−C28	-90.74	C13−N2−C19−C31	- 89.45

Table S2: Stock solution of drugs and their highest tested concentrations.

Drugs/compounds	**Stock**	**Prepared in**	**Highest tested concentration (X)**	**No. of concentration tested (y)**
CQ	25 mM	PBS (pH 7.5)	5 µM	11
1a-e	4 mM	DMSO	40 µM	20
2a-b,3	4 mM	DMSO	20 µM	20
2c	2 mM	DMSO	20 µM	20
4	6 mM	DMSO	60 µM	20
5	8 mM	DMSO	40 µM	20

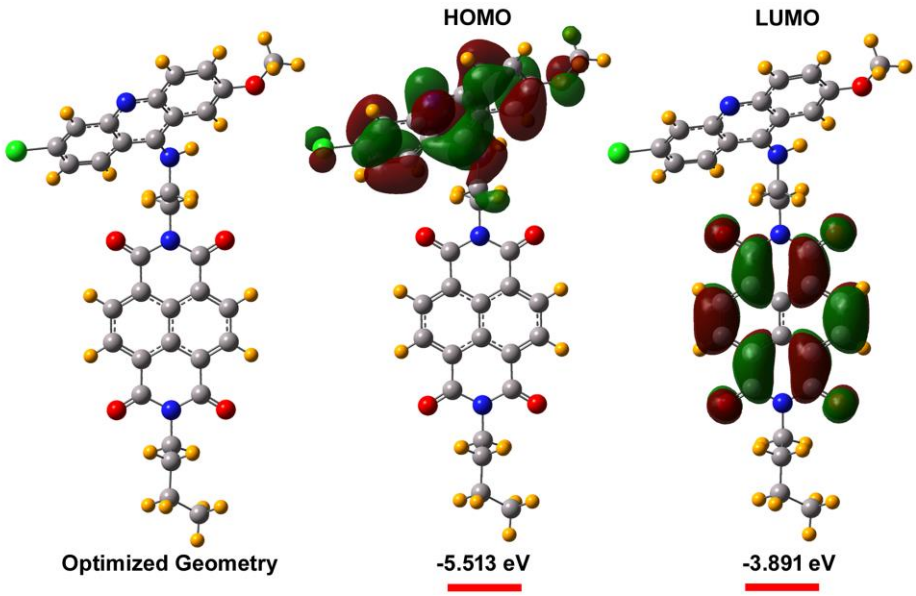

Figure S1: Electronic density contours of the HOMO (middle) and LUMO (right) of **2a.**

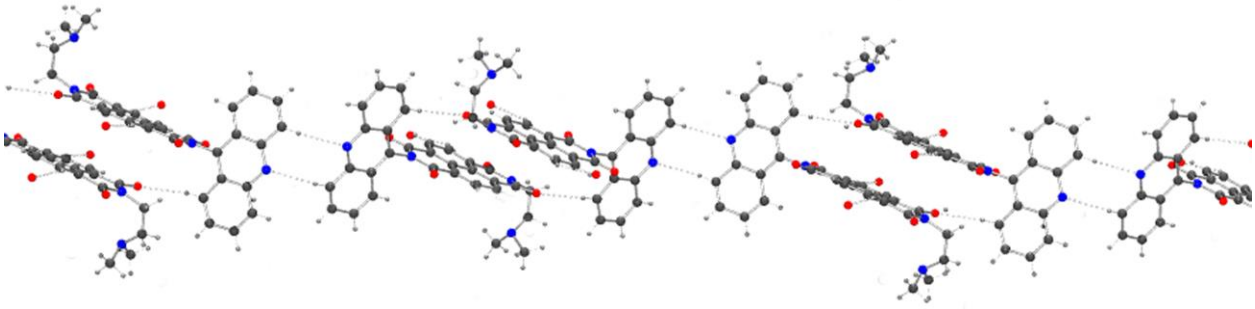

Figure S2. Self-assembled crystal lattice of compound **1b,** showing H-bonding and π-π interactions.

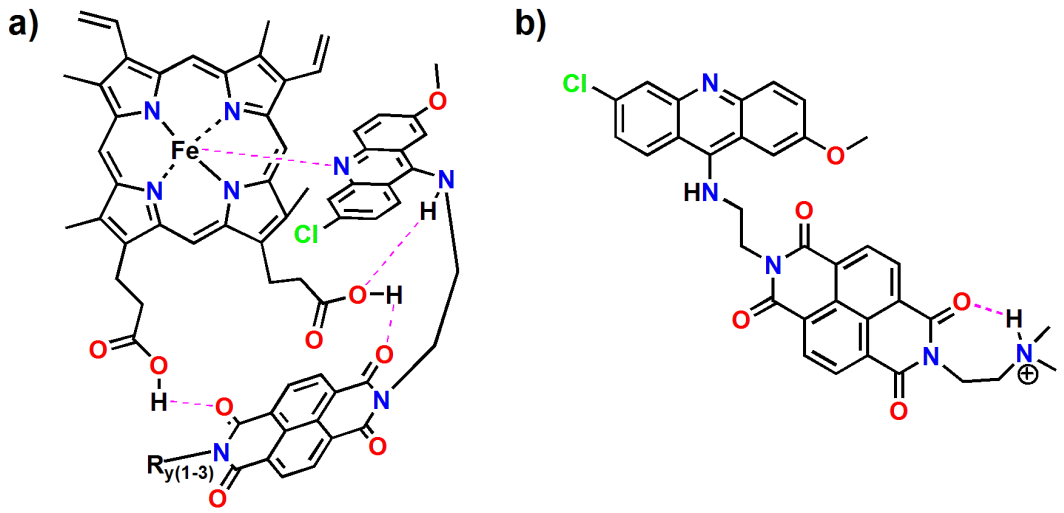

Figure S3. Proposed H-bonding model. a) Displays intermolecular H-bonding mode of heme with compounds **2a-c** to form complexes. b) Displays the intramolecular H-bonding model of compound **2b** at physiological pH.

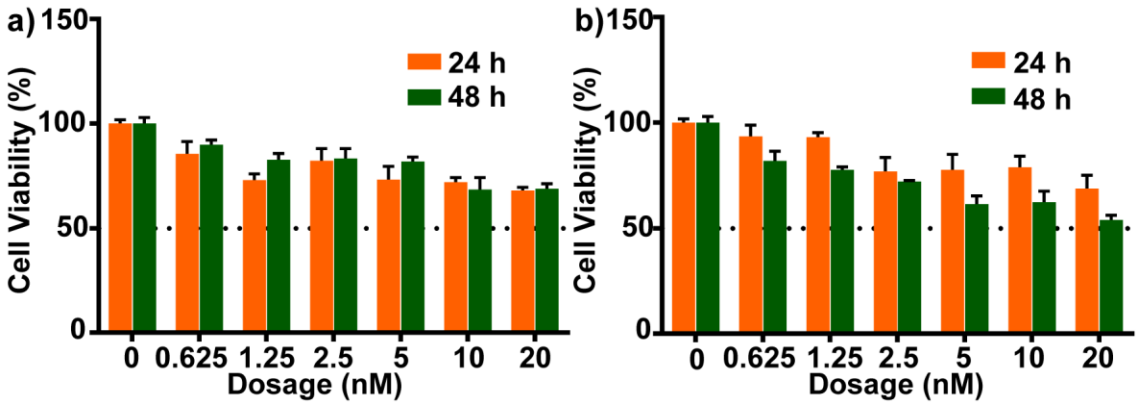

Figure S4: Viability of NIH3T3 cells treated with different concentrations of a) **2a** and b) **2b** after incubation for 24 h (orange bars) and 48 h (green bars) at 37 °C as measured by using MTT assay by monitoring formazan absorbance at 507 nm. Data are presented as mean ± SD from three independent experiments.

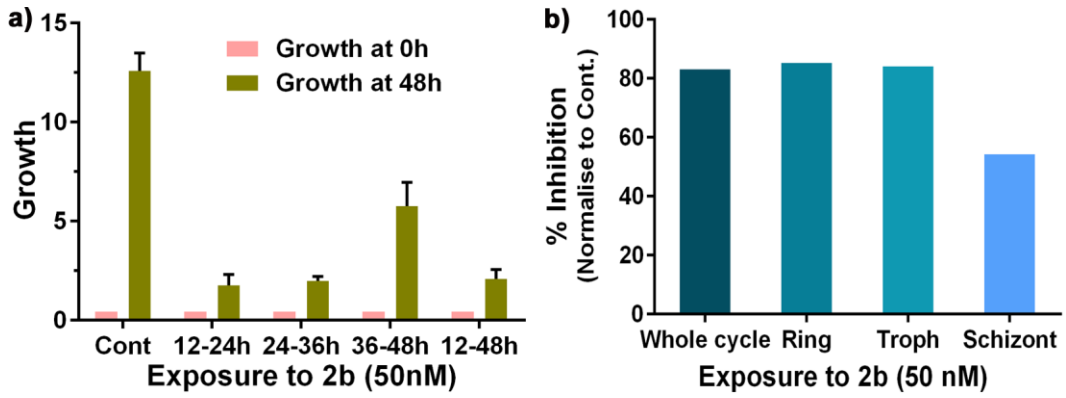

Figure S5: Effect of **2b** on different intraerythrocytic stages of malaria parasites *P. falciparum* (3D7). Highly synchronized ring (~12 h), trophozoite (~24 h), and schizont (~36 h) stages were treated with 50 nM **2b** for 12 h. After completion of treatment, parasites were washed to remove drug pressure and subsequently re-suspended in drug free media to complete the life cycle. Ring-stage parasites (~12 h) were also incubated continuously for 36 h. After completion of the first lifecycle, the growth of the parasites was determined by fluorescence based SYBR Green I assay. a) Growth of different intraerythrocytic stages treated with **2b**. b) Percentage of inhibition of growth of different intraerythrocytic stages treated with **2b**. Data are presented as mean ± SEM from three independent experiments.

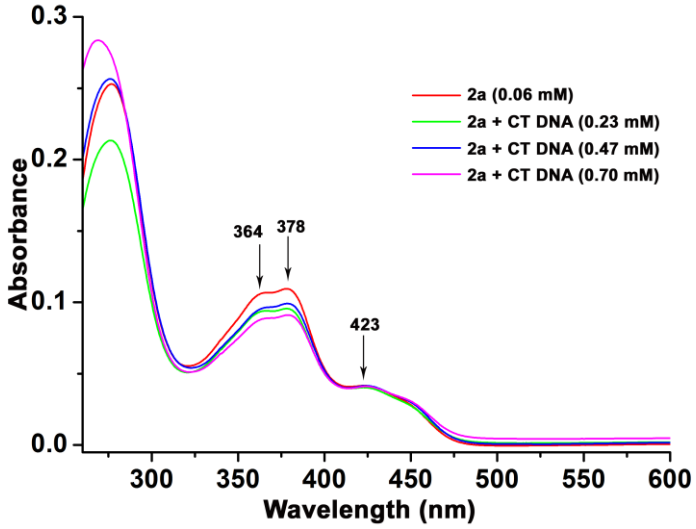

Figure S6: UV-Visible spectral changes upon titration of **2a** (0.06 mM) with CT DNA (0-0.70 mM) in buffered MeOH [3 : 1/ MeOH : TE buffer (pH 8)].

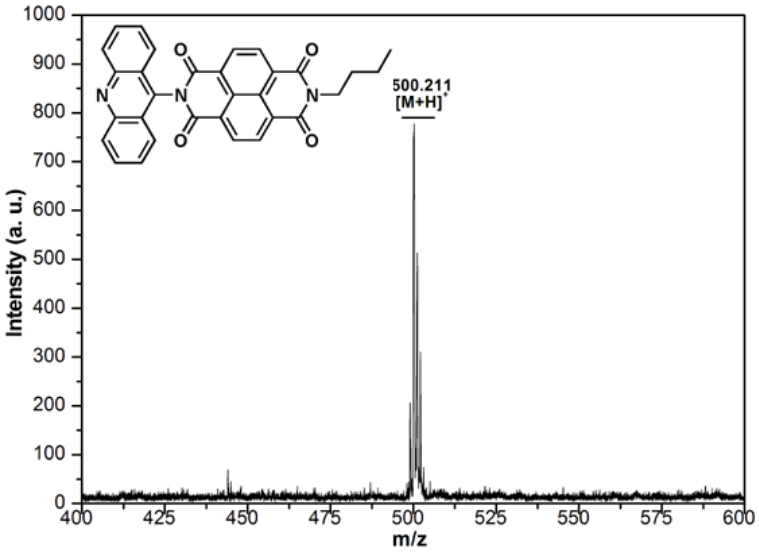

Figure S7: MALDI-TOF mass spectrum of **1a**.

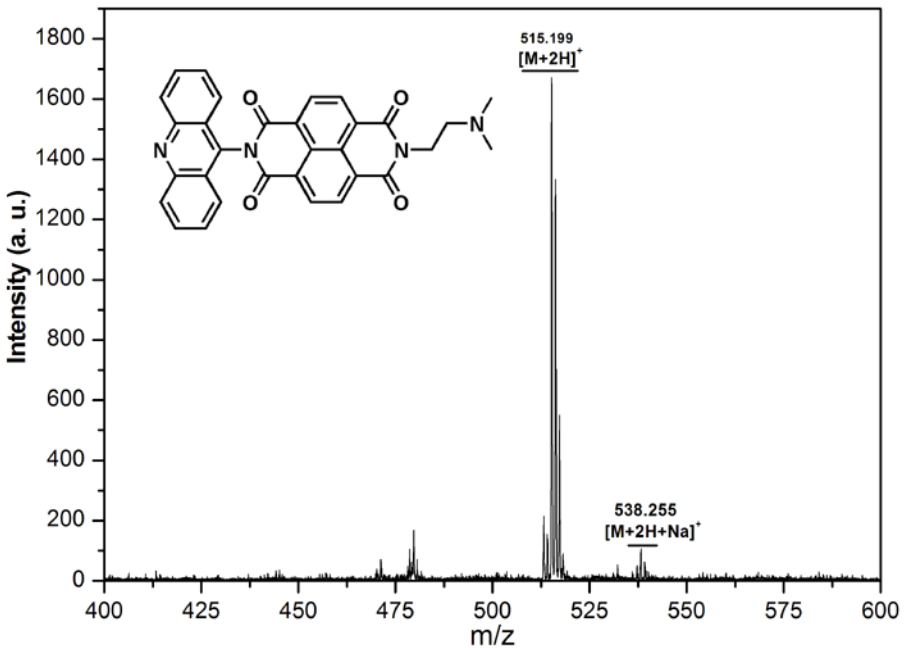

Figure S8: MALDI-TOF mass spectrum of **1b**.

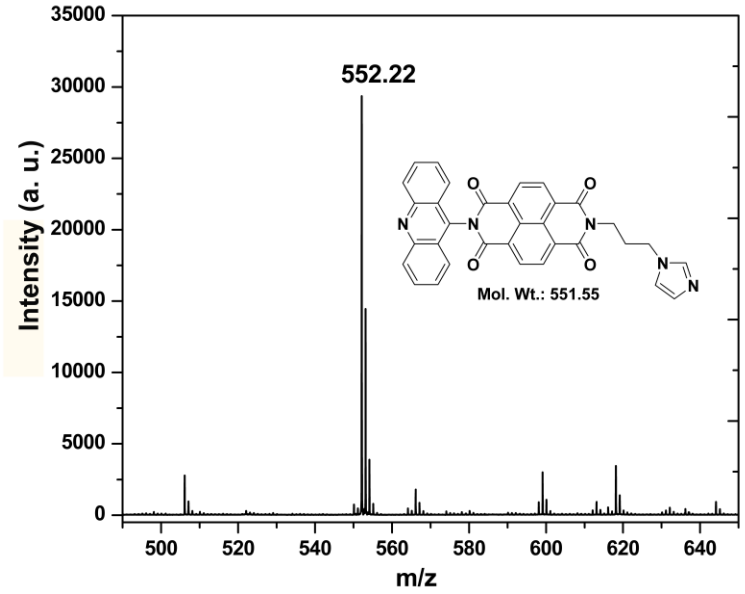

Figure S9: MALDI-TOF mass spectrum of **1c**.

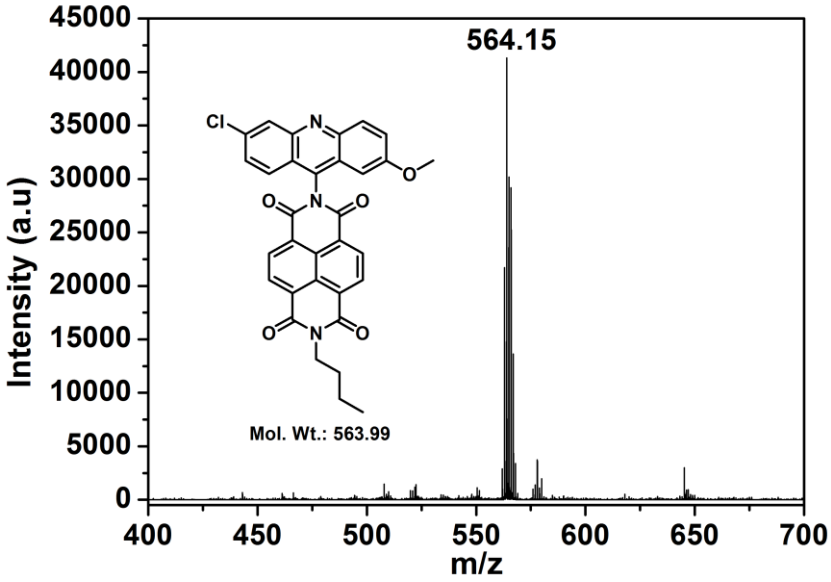

Figure S10: MALDI-TOF mass spectrum of **1d**.

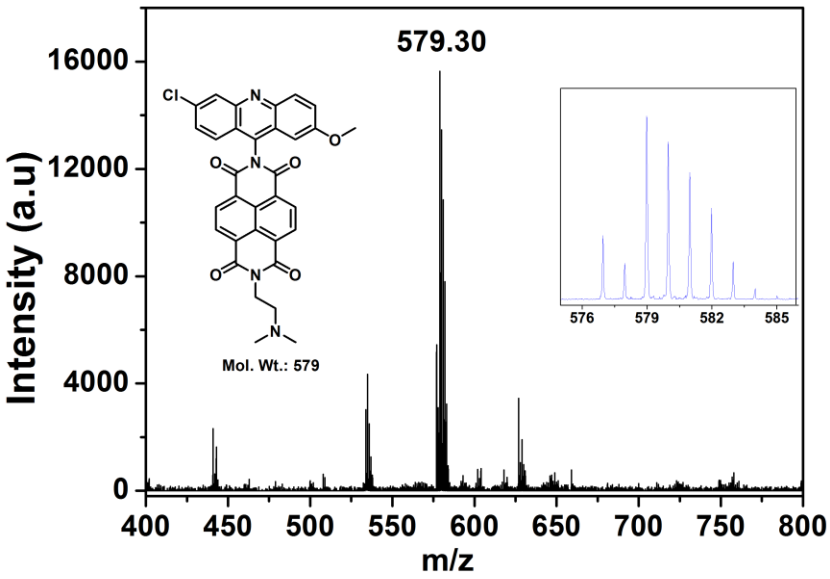

Figure S11: MALDI-TOF mass spectrum of **1e**.

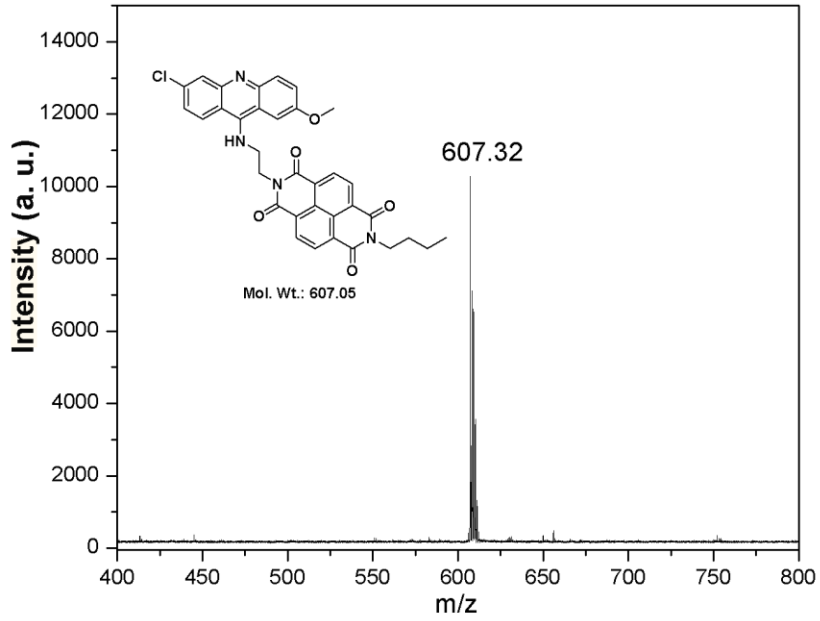

Figure S12: MALDI-TOF mass spectrum of **2a**.

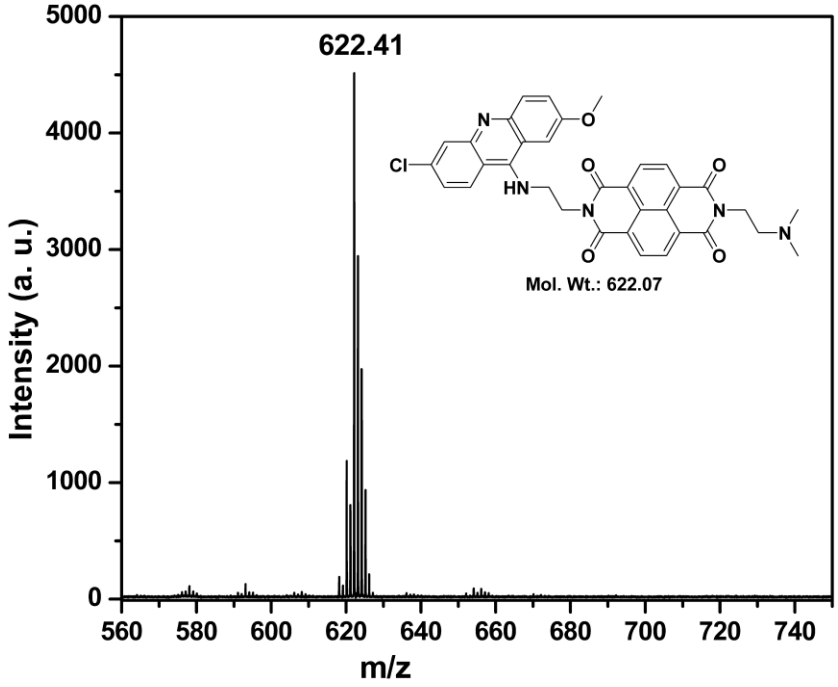

Figure S13: MALDI-TOF mass spectrum of **2b**.

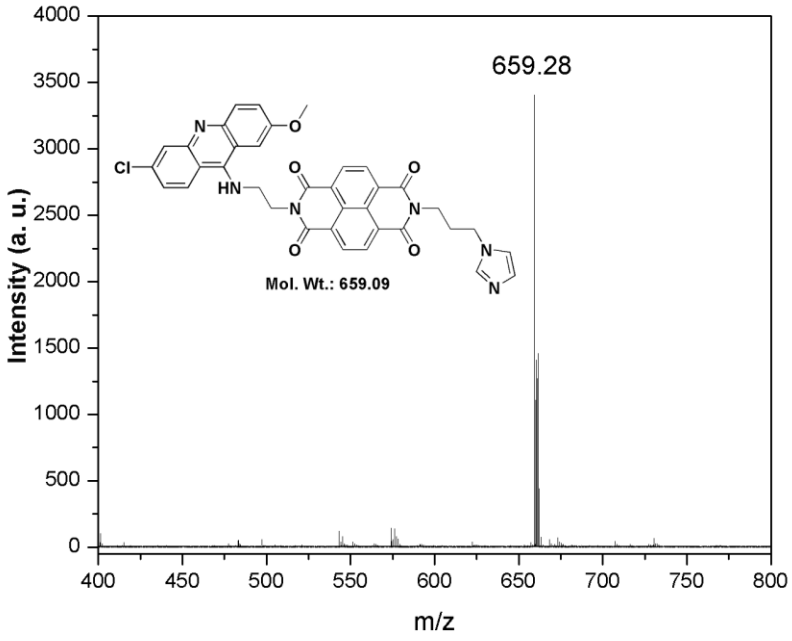

Figure S14: MALDI-TOF mass spectrum of **2c**.

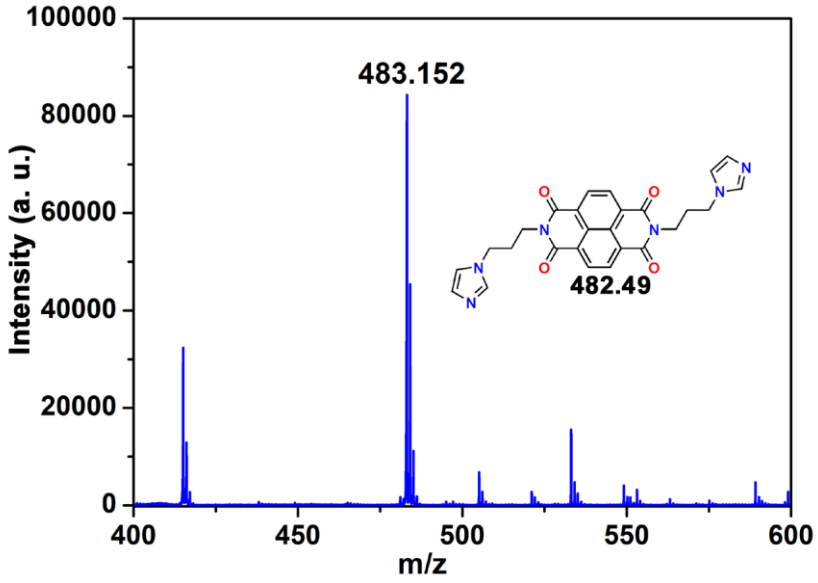

Figure S15: MALDI-TOF mass spectrum of **4**.

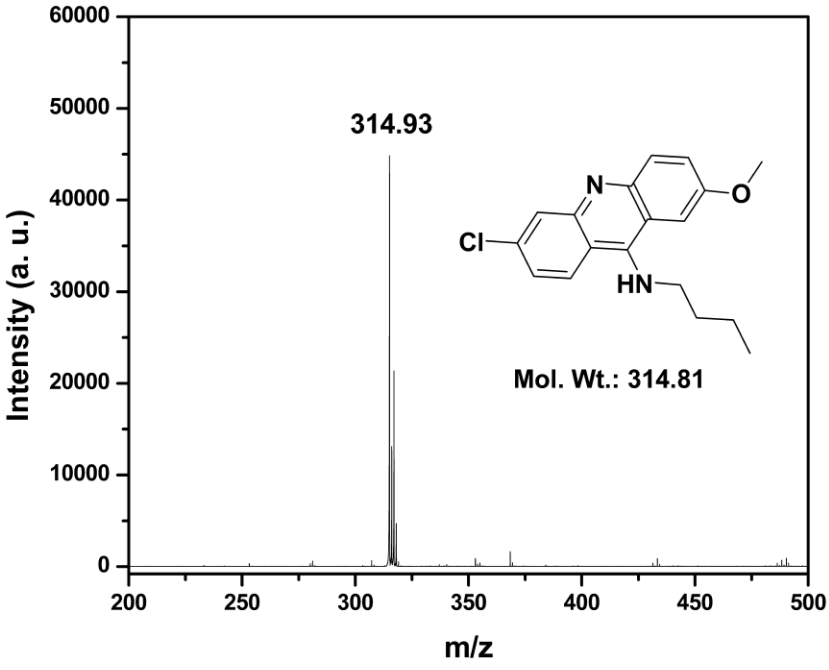

Figure S16: MALDI-TOF mass spectrum of **5**.

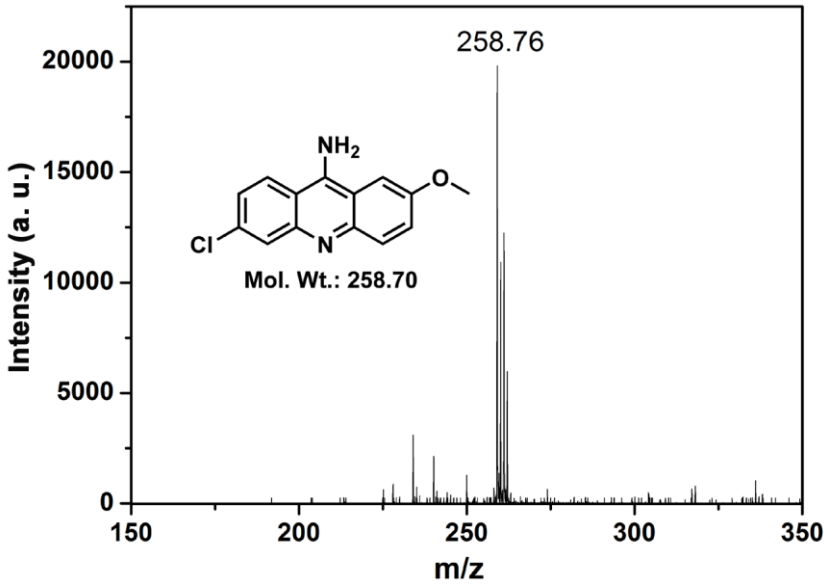

Figure S17: MALDI-TOF mass spectrum of **6**.

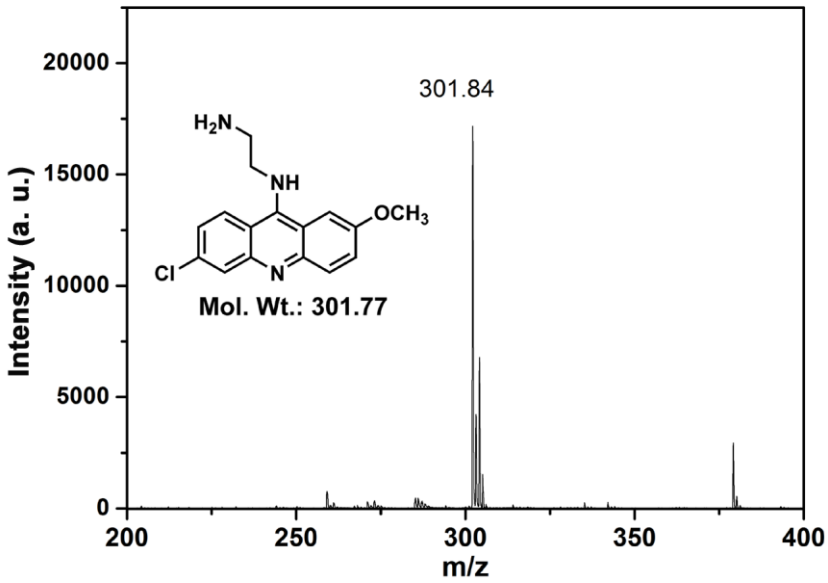

Figure S18: MALDI-TOFF mass spectrum of **7**.

.

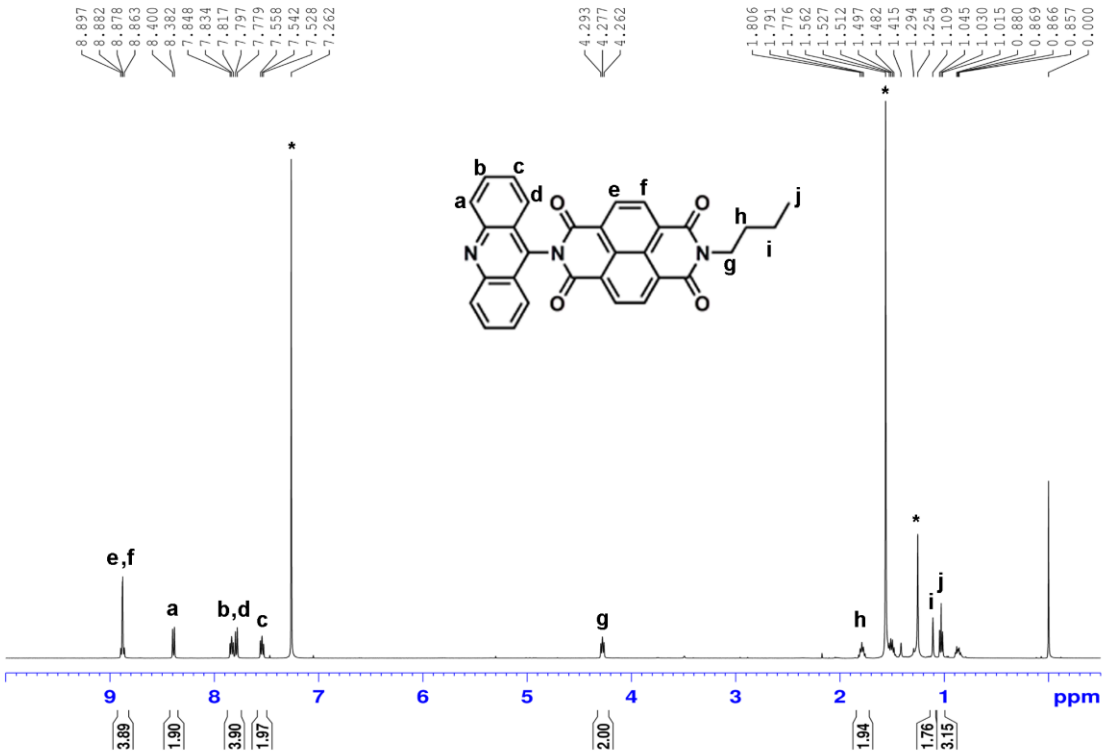

Figure S19: 500 MHz ^{1}HNMR spectrum of **1a** in $CDCl_3$ at room temperature.

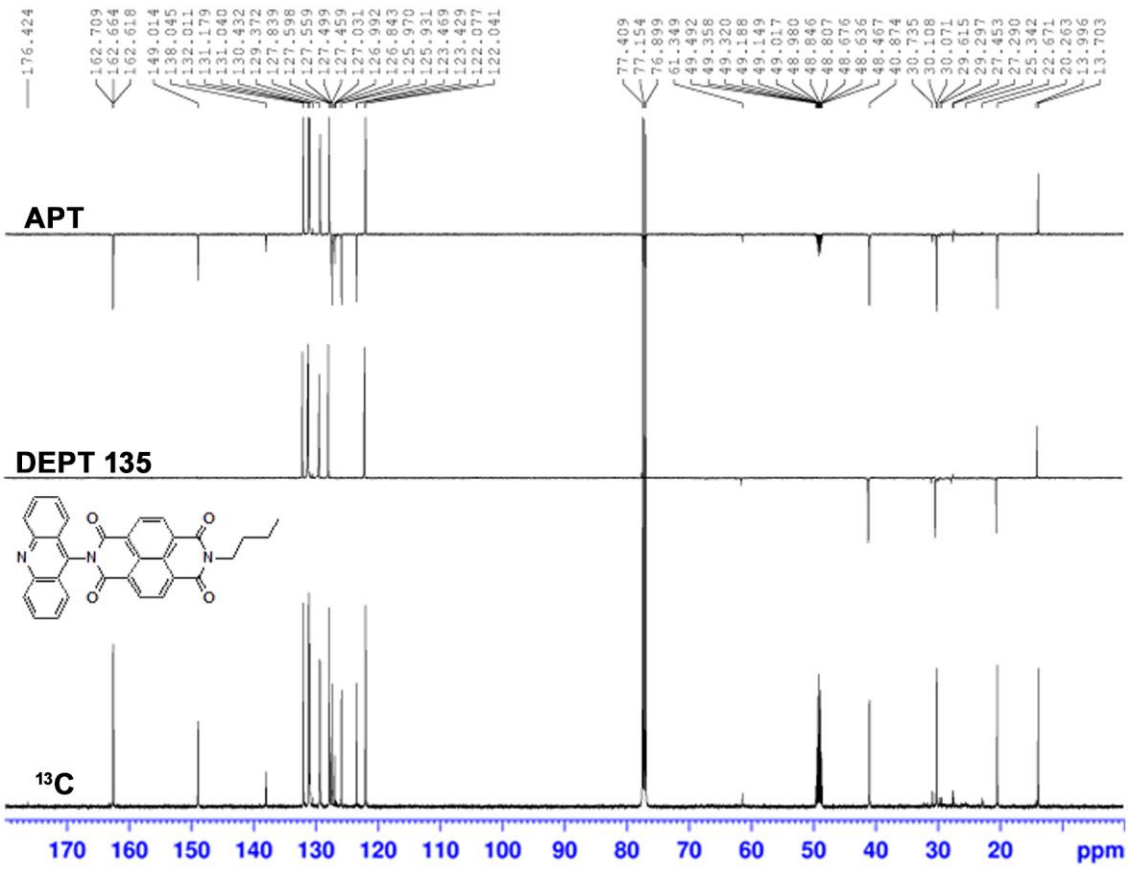

Figure S20: 125 MHz ^{13}C, DEPT-135 and APT spectra of **1a** in $CDCl_3$ at room temperature.

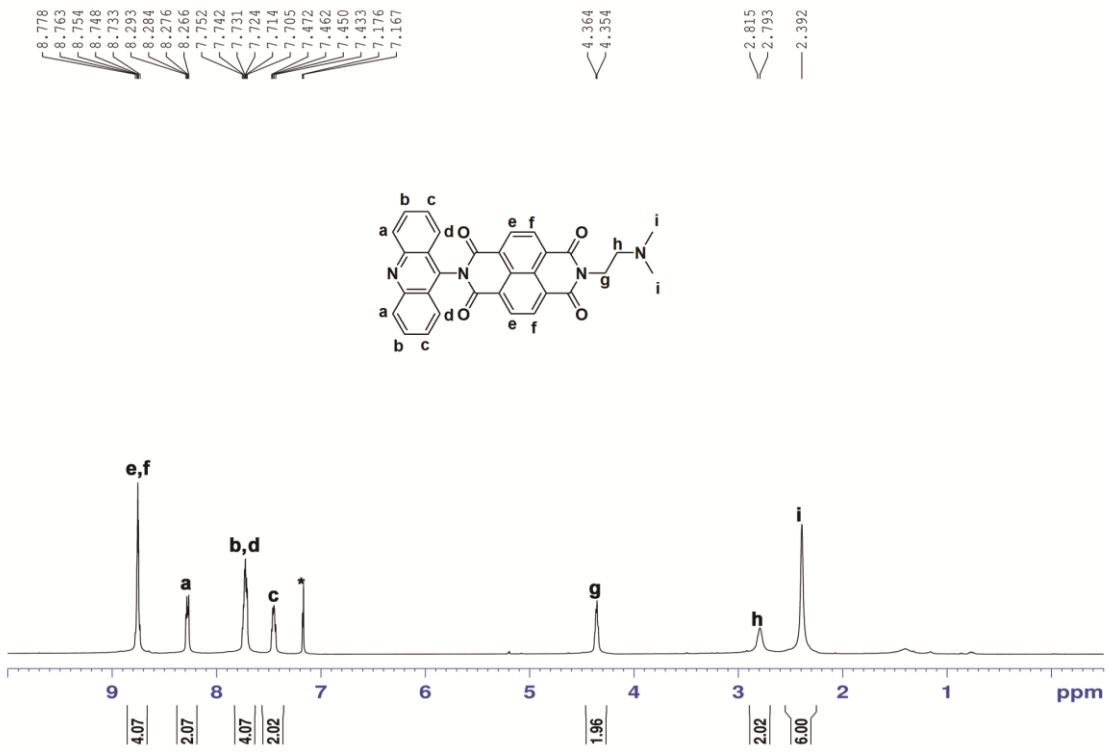

Figure S21: 500 MHz ^{1}HNMR spectrum of **1b** in $CDCl_3$ at room temperature.

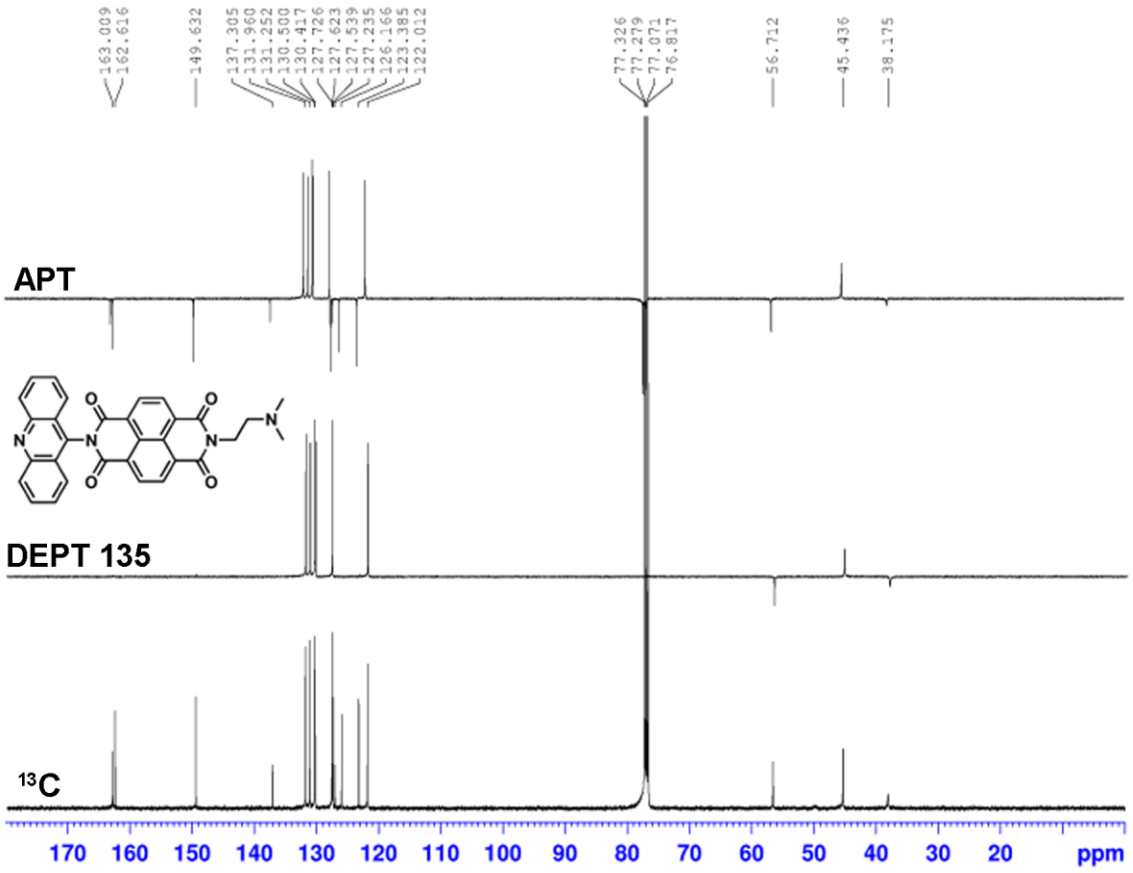

Figure S22: 125 MHz ^{13}C, DEPT-135 and APT spectra of **1b** in $CDCl_3$ at room temperature.

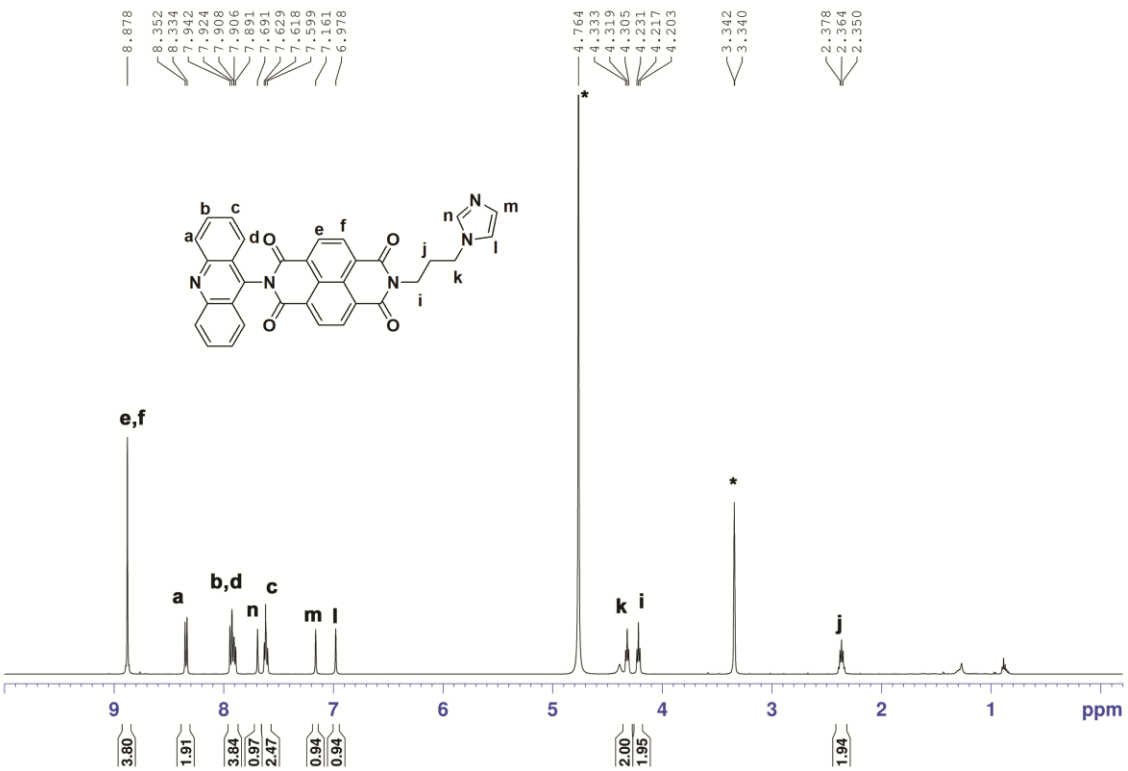

Figure S23: 500 MHz ^{1}HNMR spectrum of **1c** in MeOD at room temperature.

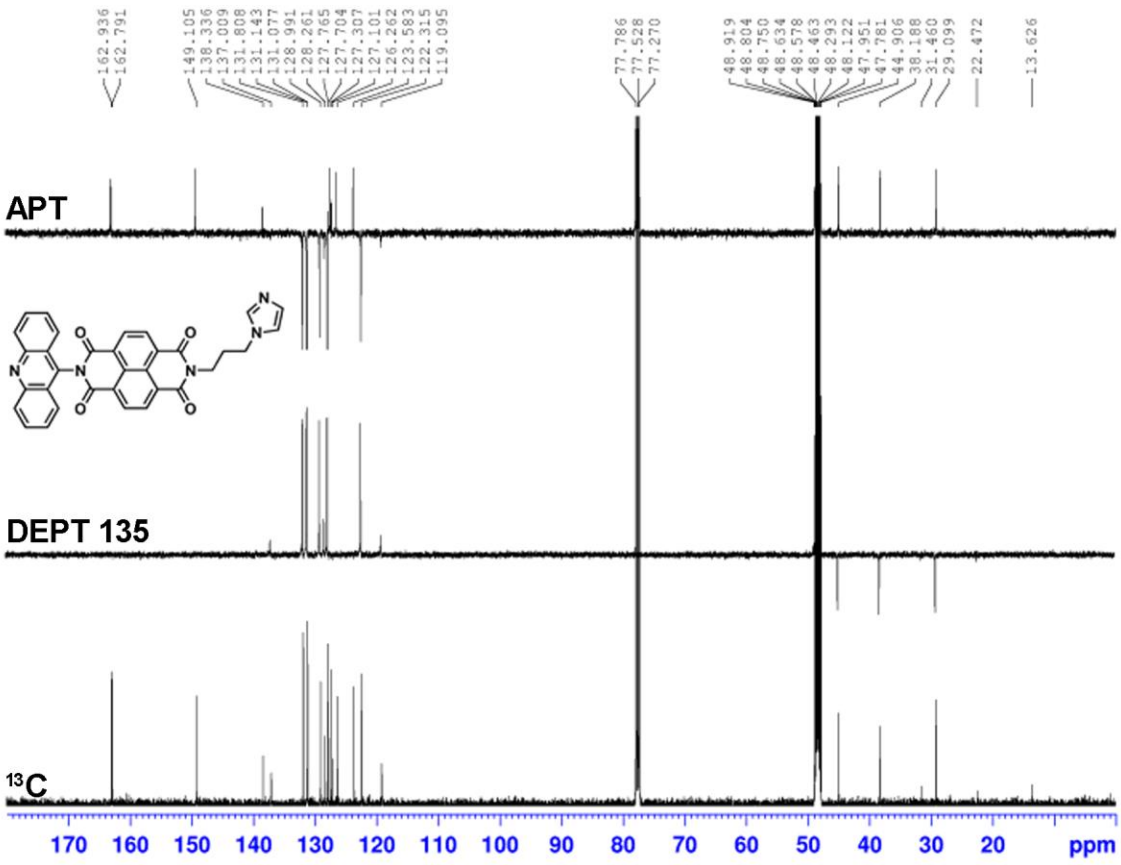

Figure S24: 125 MHz ^{13}C, DEPT-135 and APT spectra of **1c** in $CDCl_3$ at room temperature.

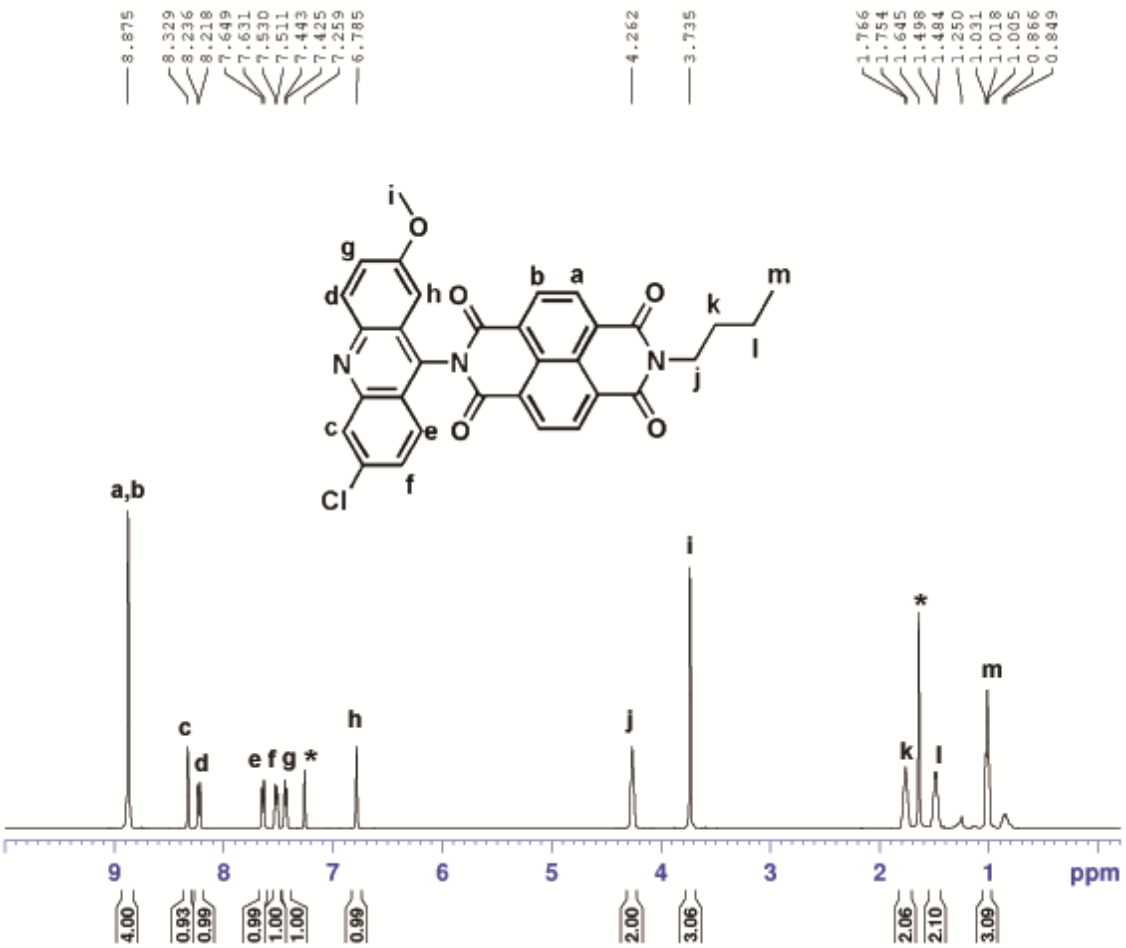

Figure S25: 500 MHz ^{1}HNMR spectrum of **1d** in $CDCl_3$ at room temperature.

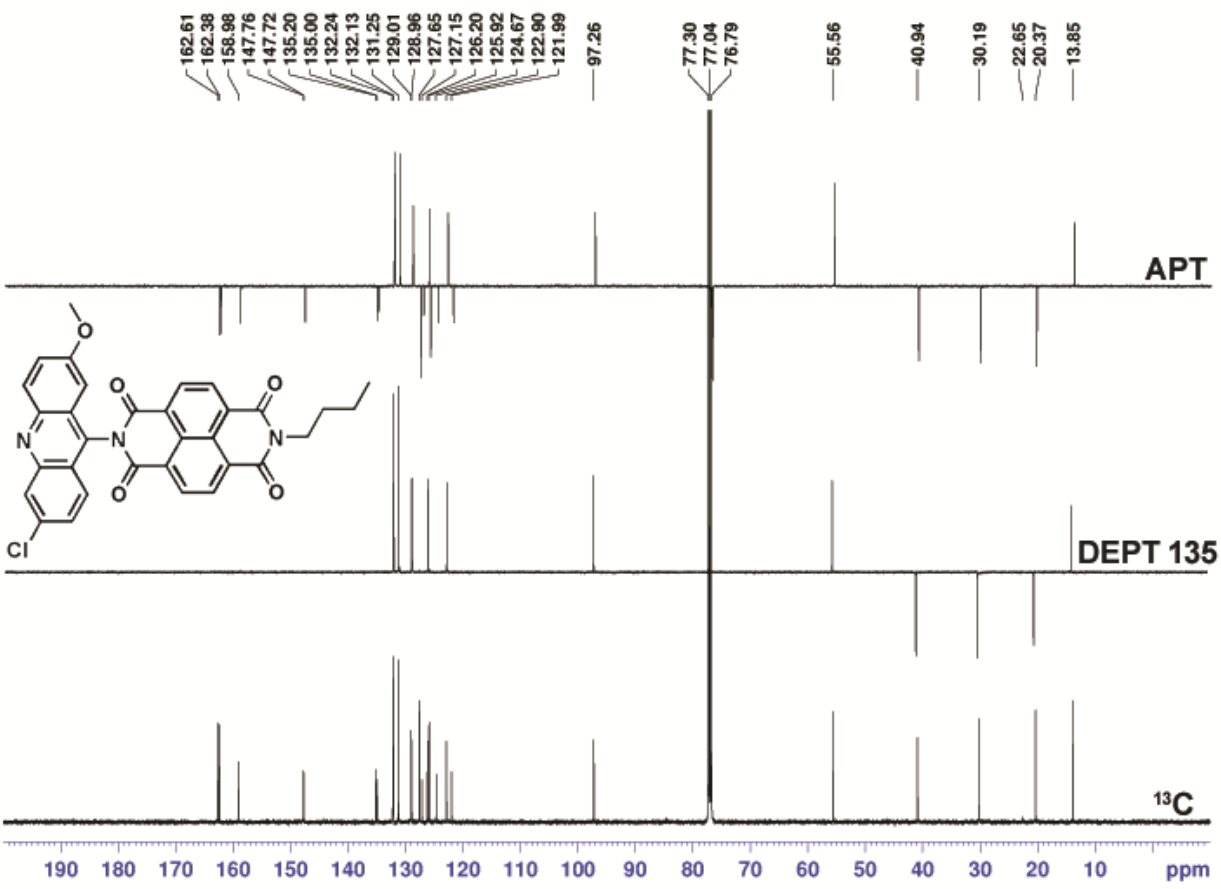

Figure S26: 125 MHz ^{13}C, DEPT-135 and APT spectra of **1d** in $CDCl_3$ at room temperature.

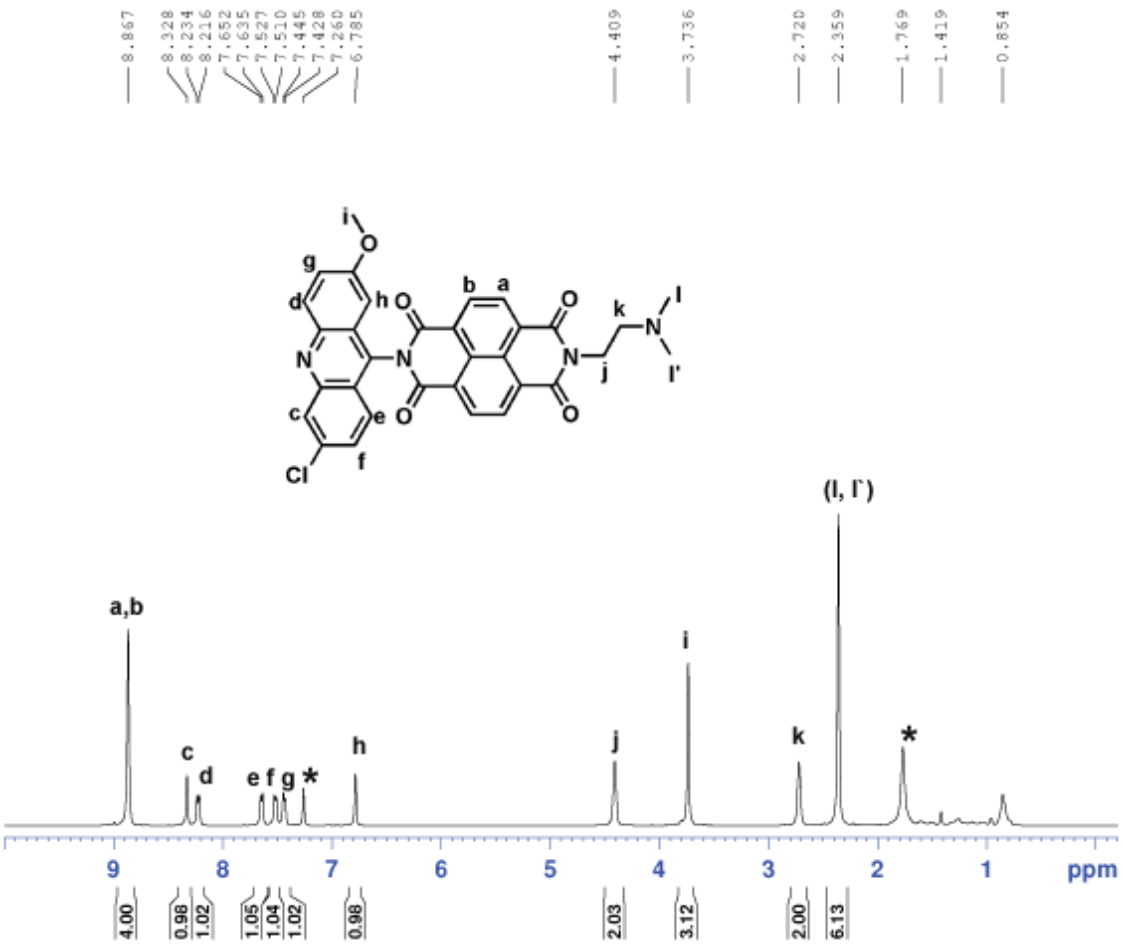

Figure S27: 500 MHz ^{1}HNMR spectrum of **1e** in $CDCl_3$ at room temperature.

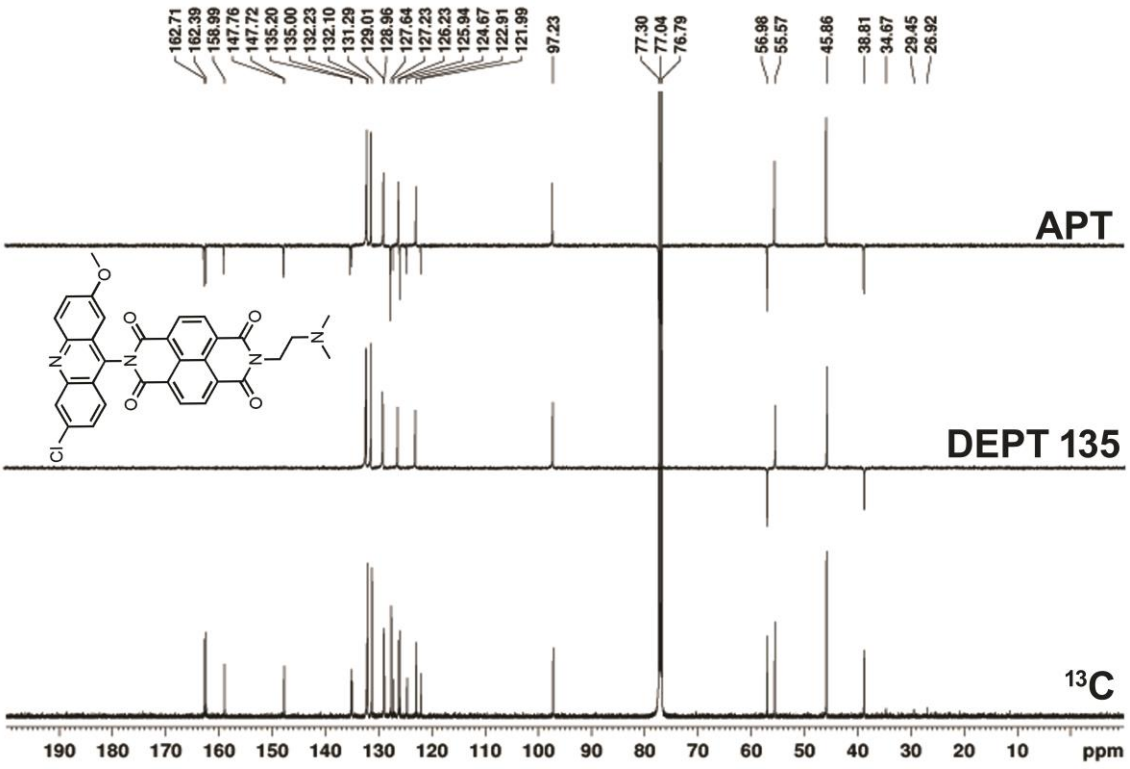

Figure S28: 125 MHz ^{13}C, DEPT-135 and APT spectra of **1e** in $CDCl_3$ at room temperature.

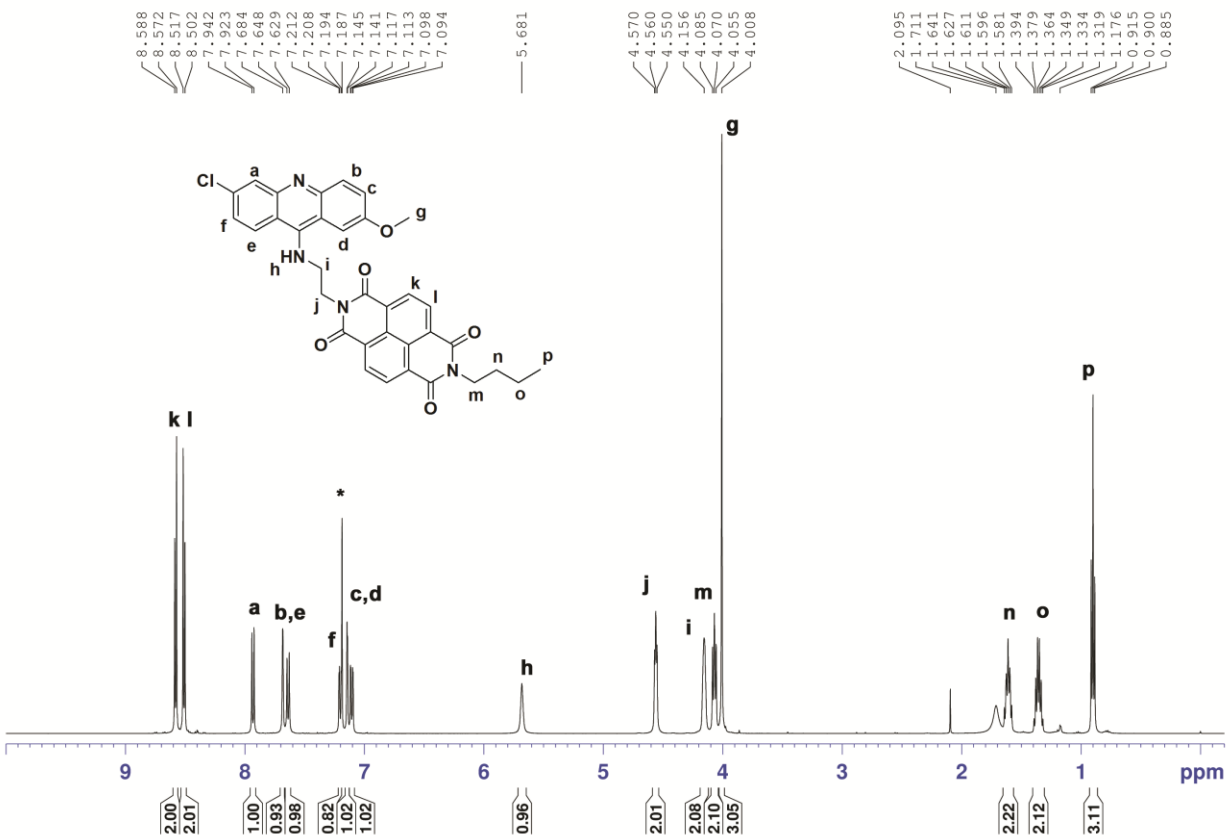

Figure S29: 500 MHz ^{1}HNMR spectrum of **2a** in $CDCl_3$ at room temperature.

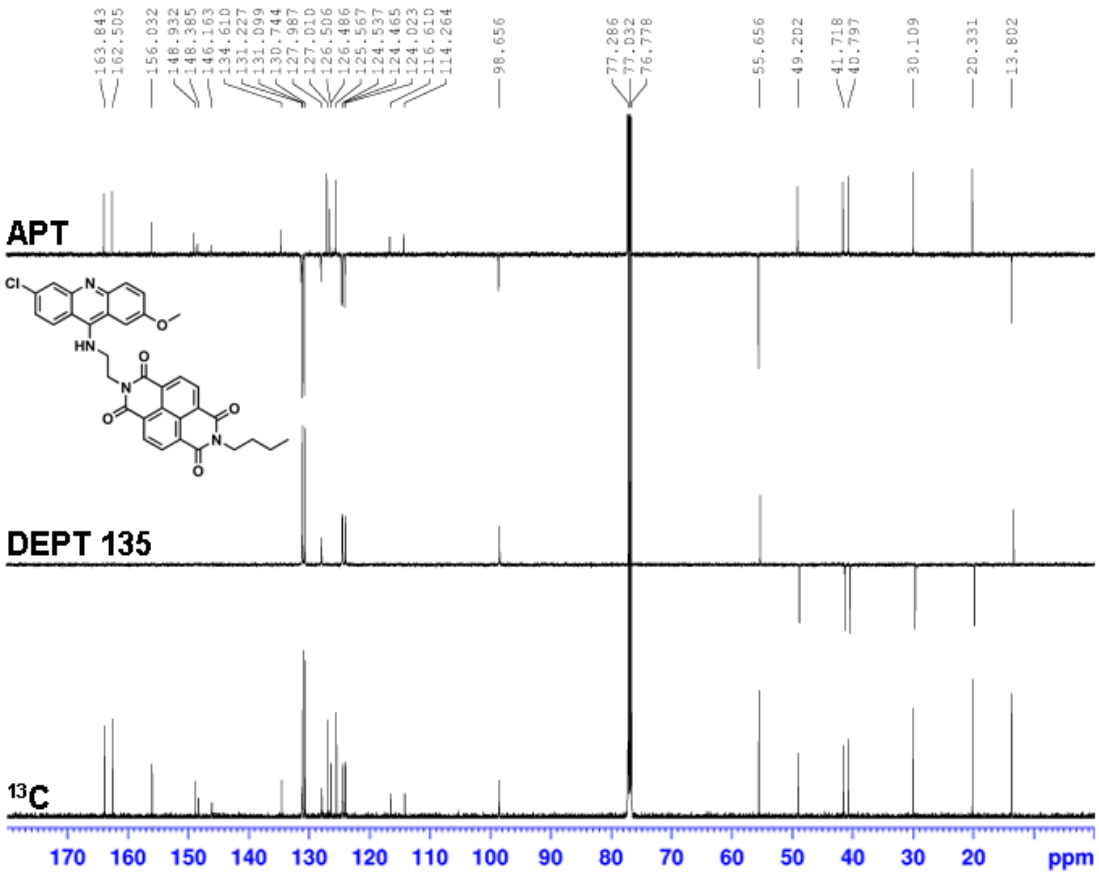

Figure S30: 125 MHz ^{13}C, DEPT-135 and APT spectra of **2a** in $CDCl_3$ at room temperature.

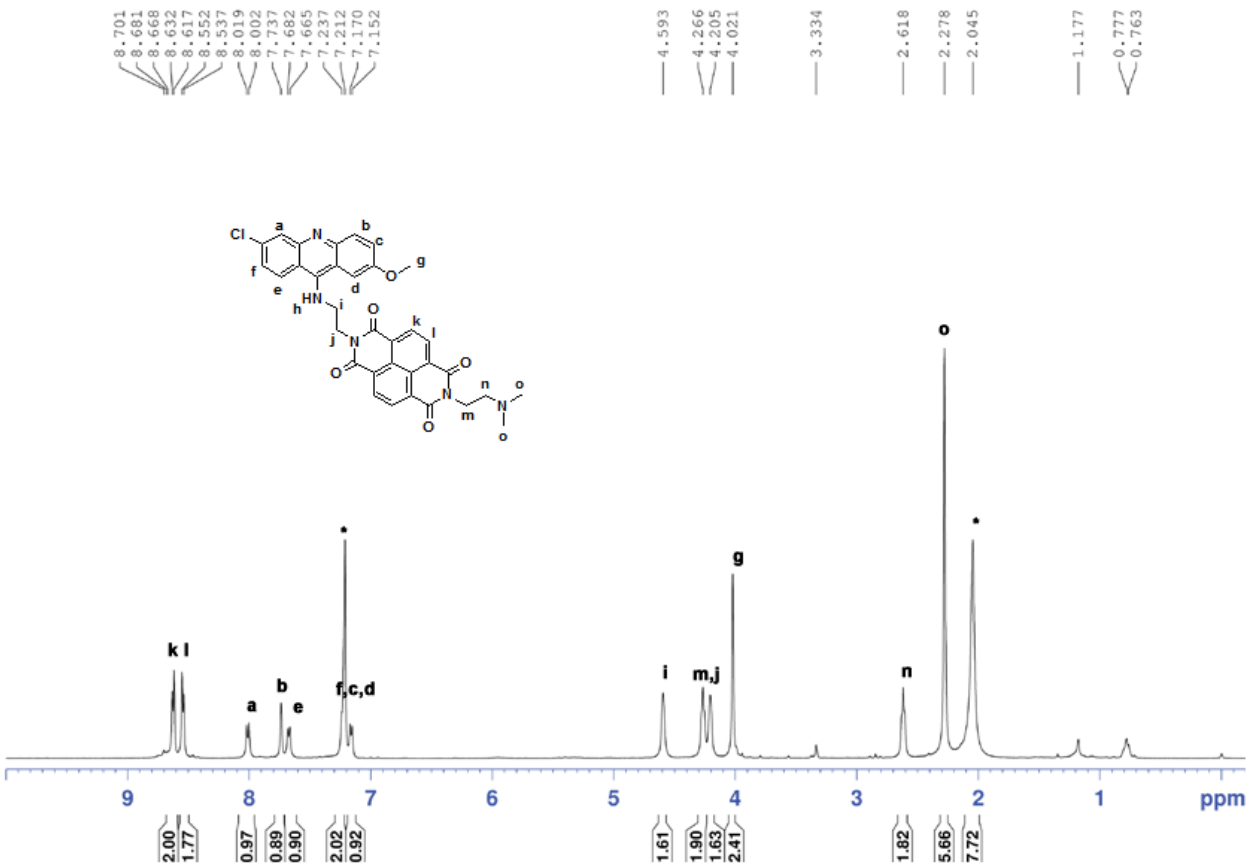

Figure S31: 500 MHz ^{1}HNMR spectrum of **2b** in $CDCl_3$ at room temperature.

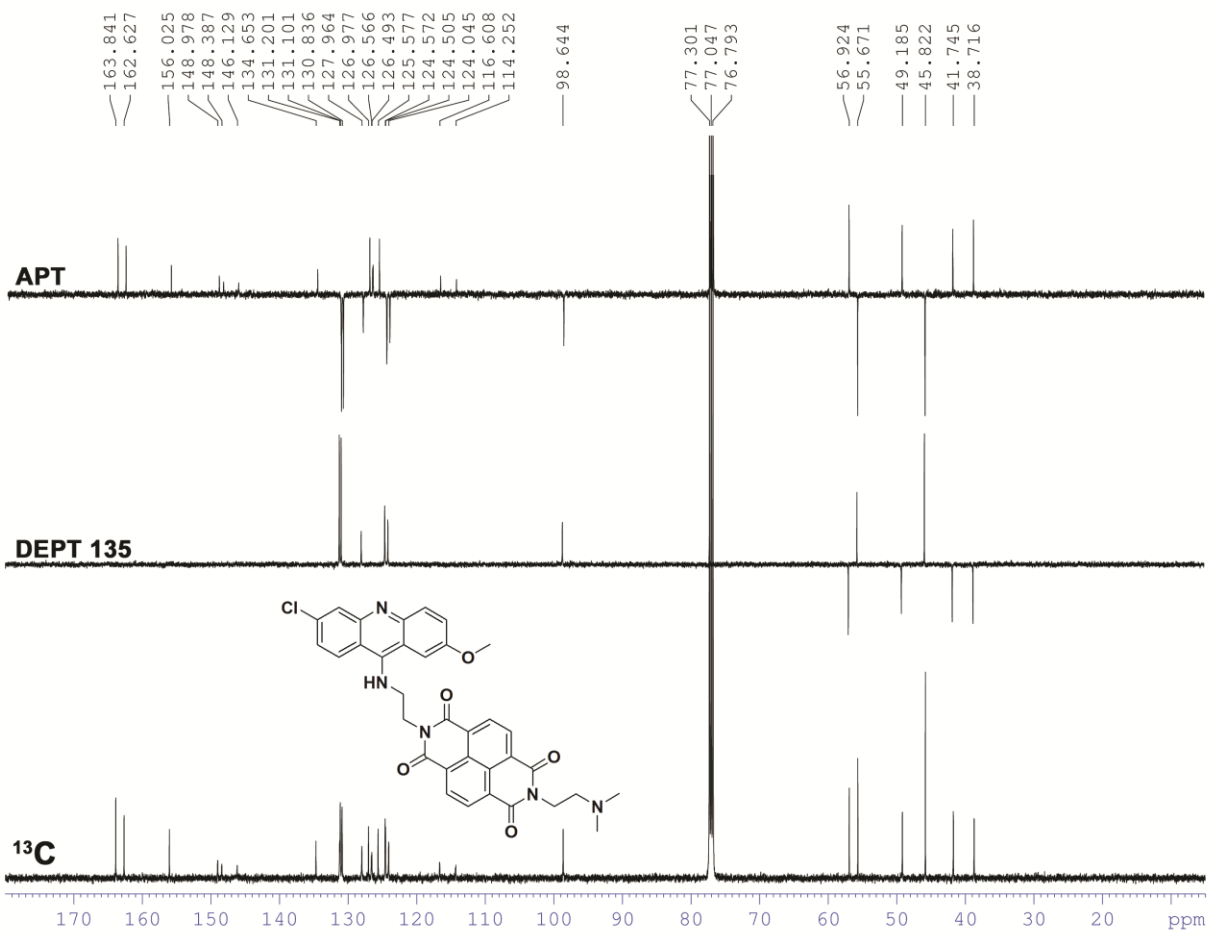

Figure S32: 125 MHz ^{13}C, DEPT-135 and APT spectra of **2b** in $CDCl_3$ at room temperature.

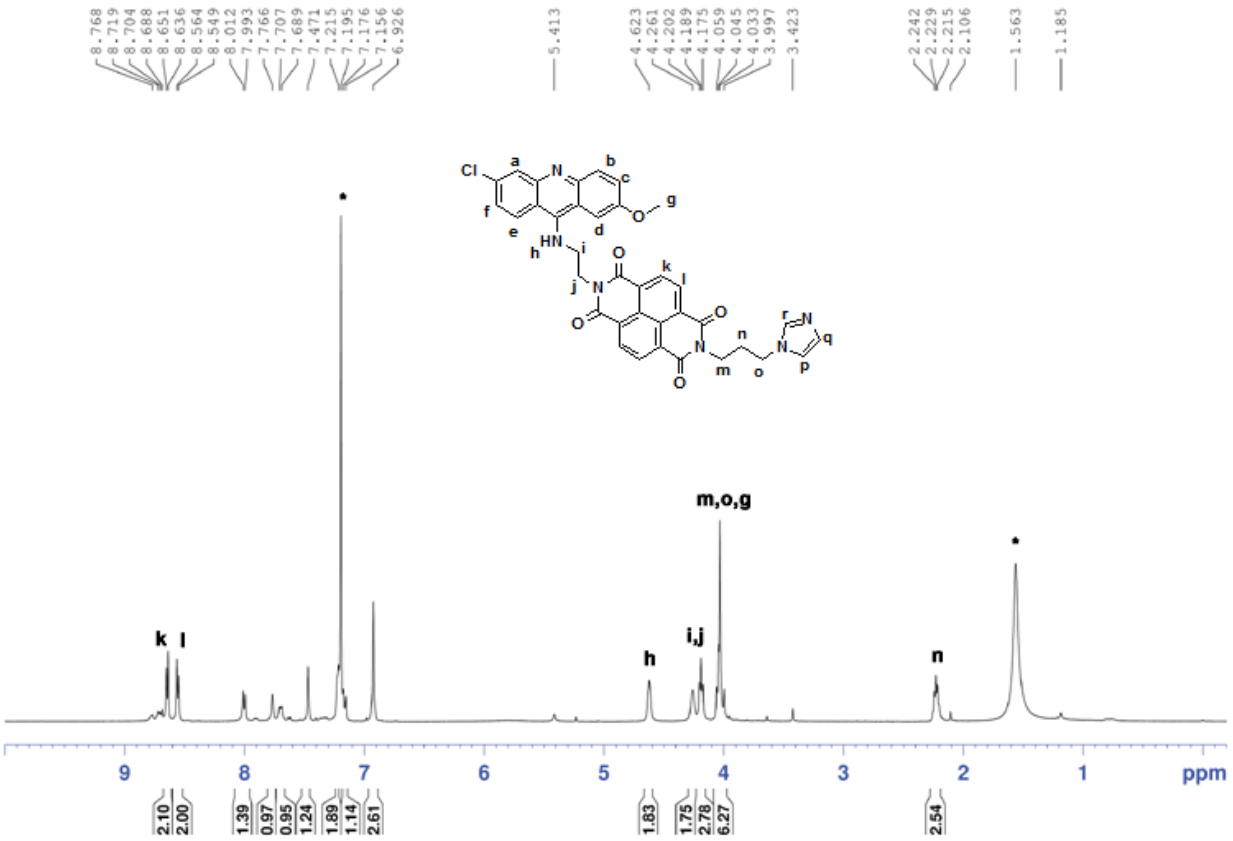

Figure S33: 500 MHz ^{1}HNMR spectrum of **2c** in $CDCl_3$ at room temperature.

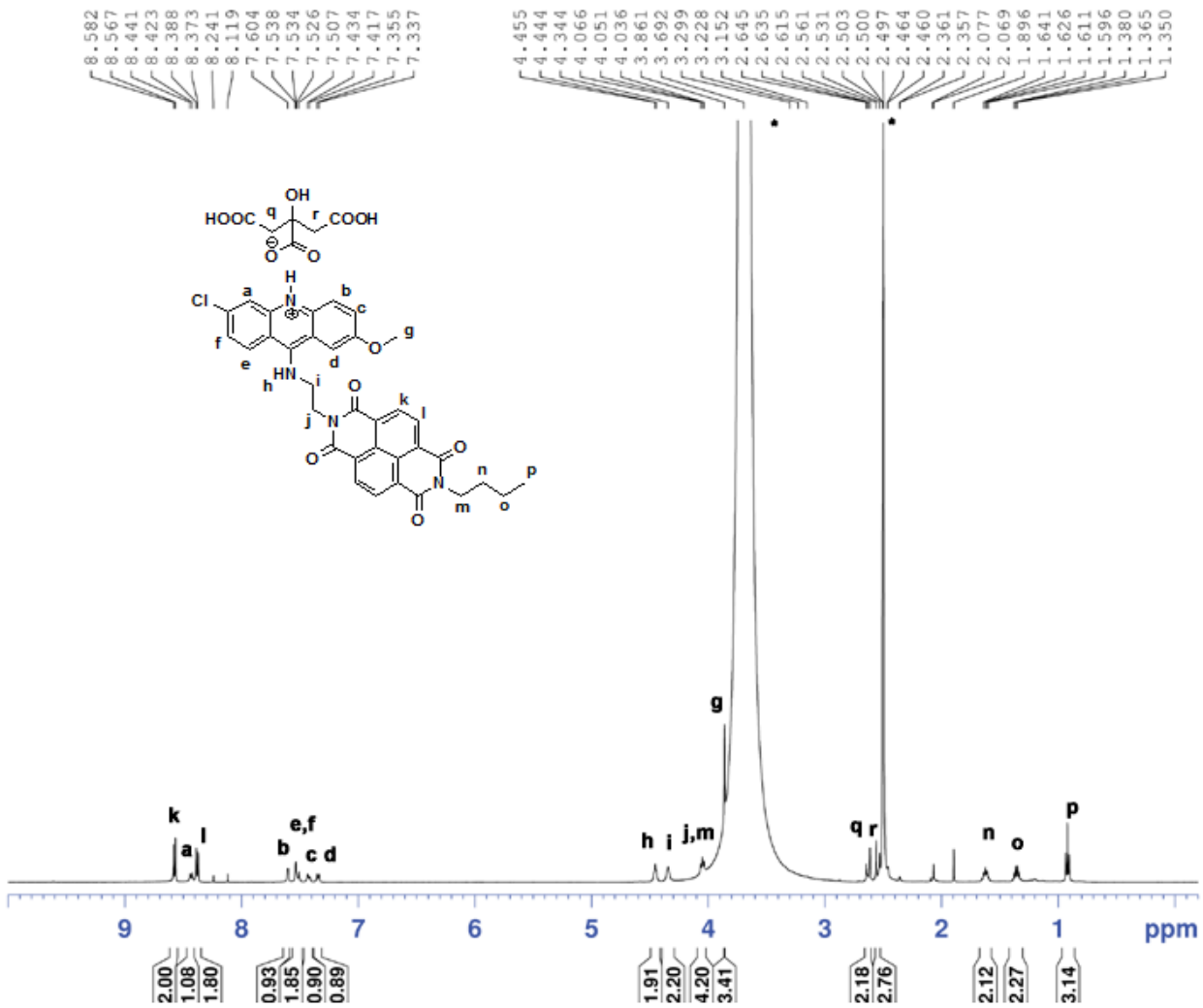

Figure S34: 500 MHz ^{1}HNMR spectrum of **3** in DMSO-d_6 at room temperature.

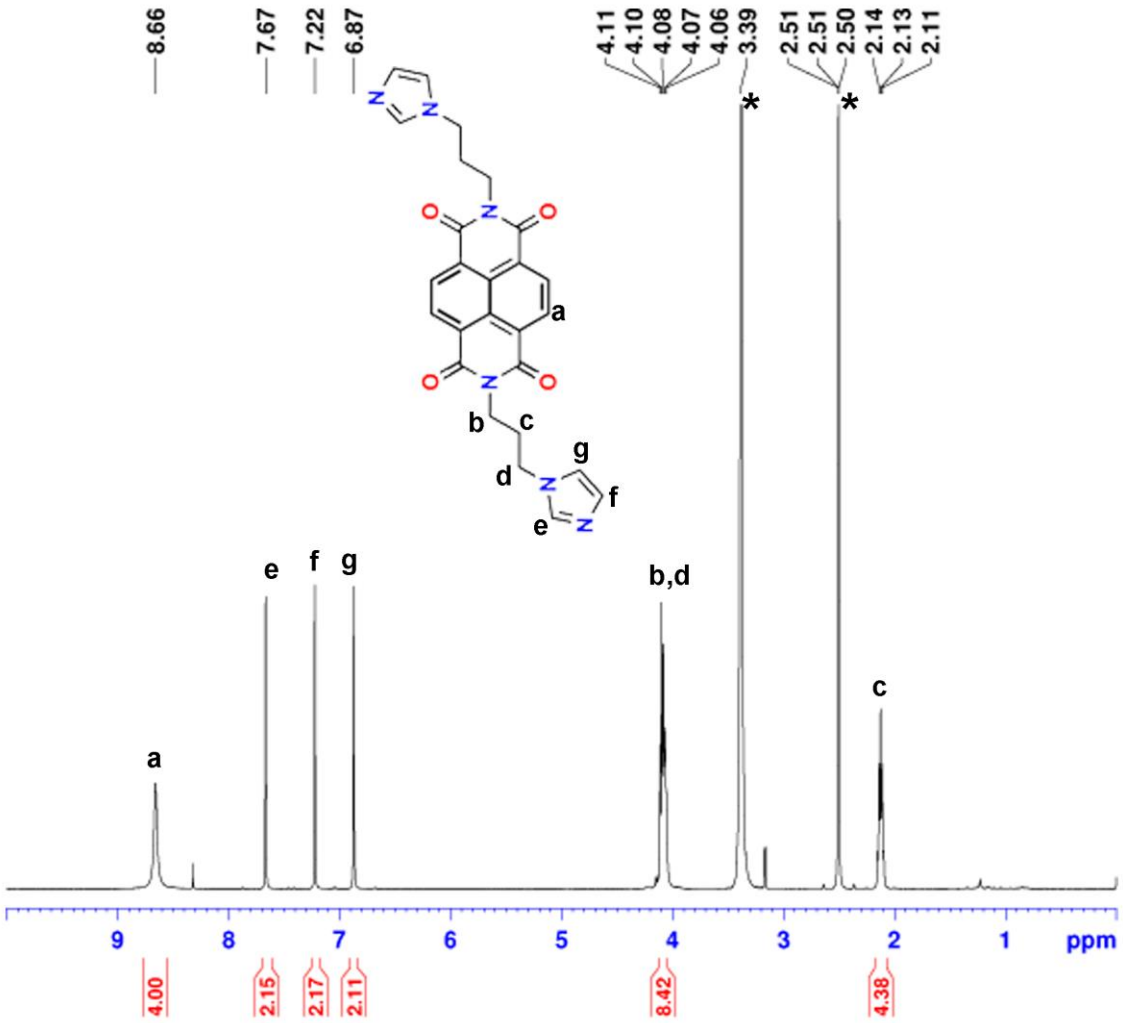

Figure S35: 500 MHz ^{1}HNMR spectrum of **4** in DMSO-d_6 at room temperature.

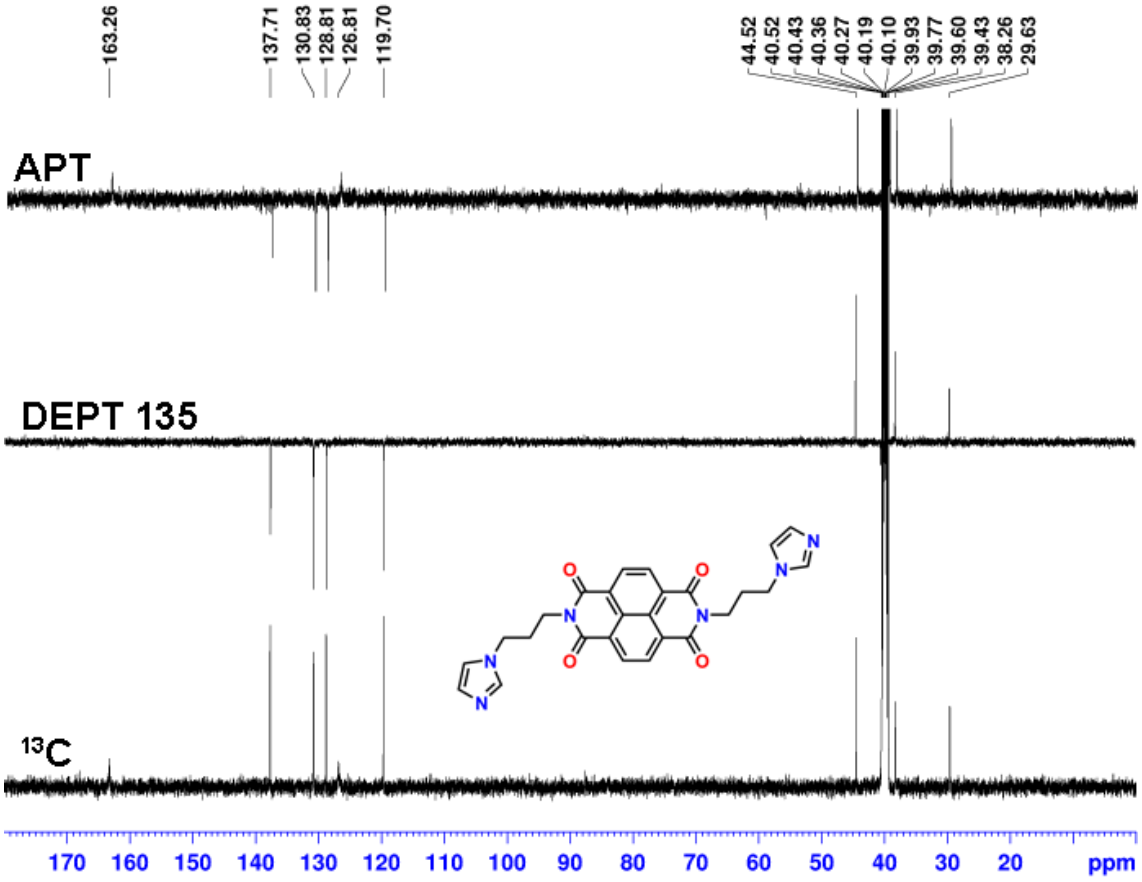

Figure S36: 125 MHz ^{13}C, DEPT-135 and APT spectra of **4** in DMSO-d_6 at room temperature.

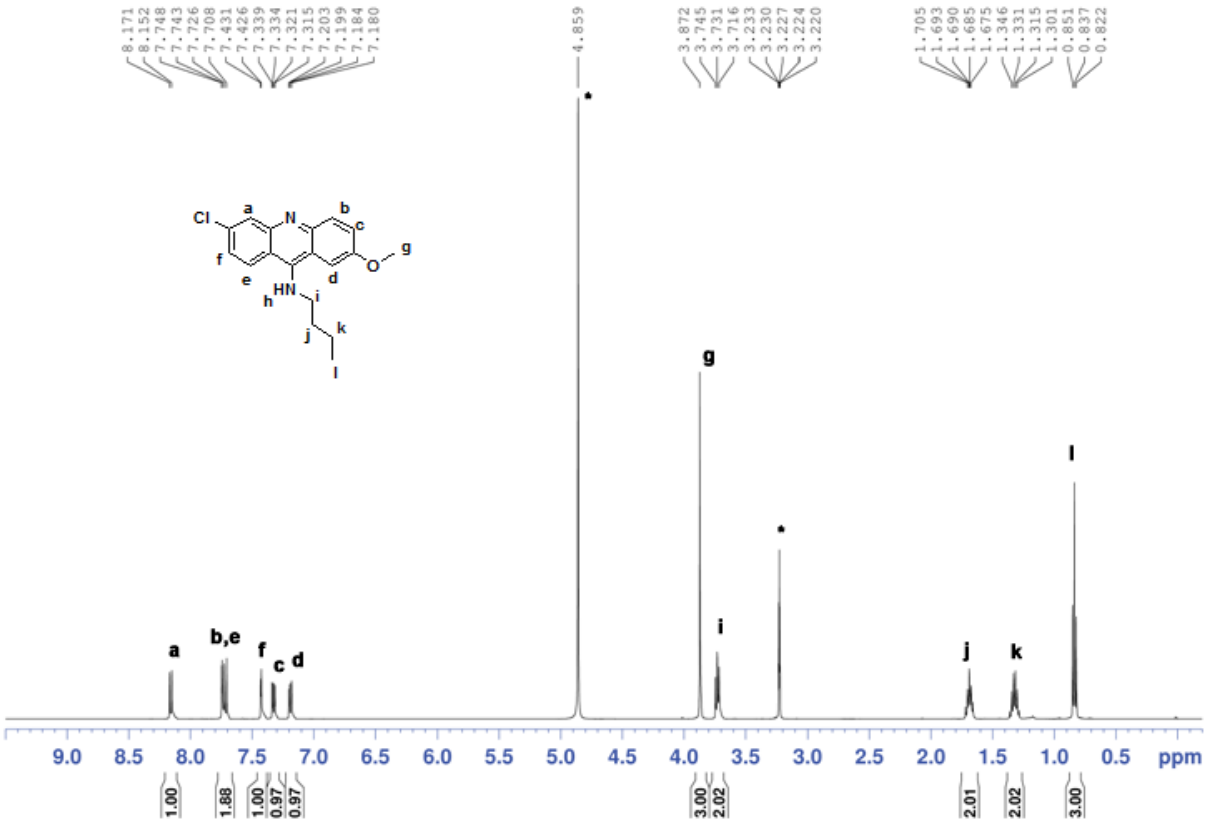

Figure S37: 500 MHz ^{1}HNMR spectrum of **5** in MeOD at room temperature.

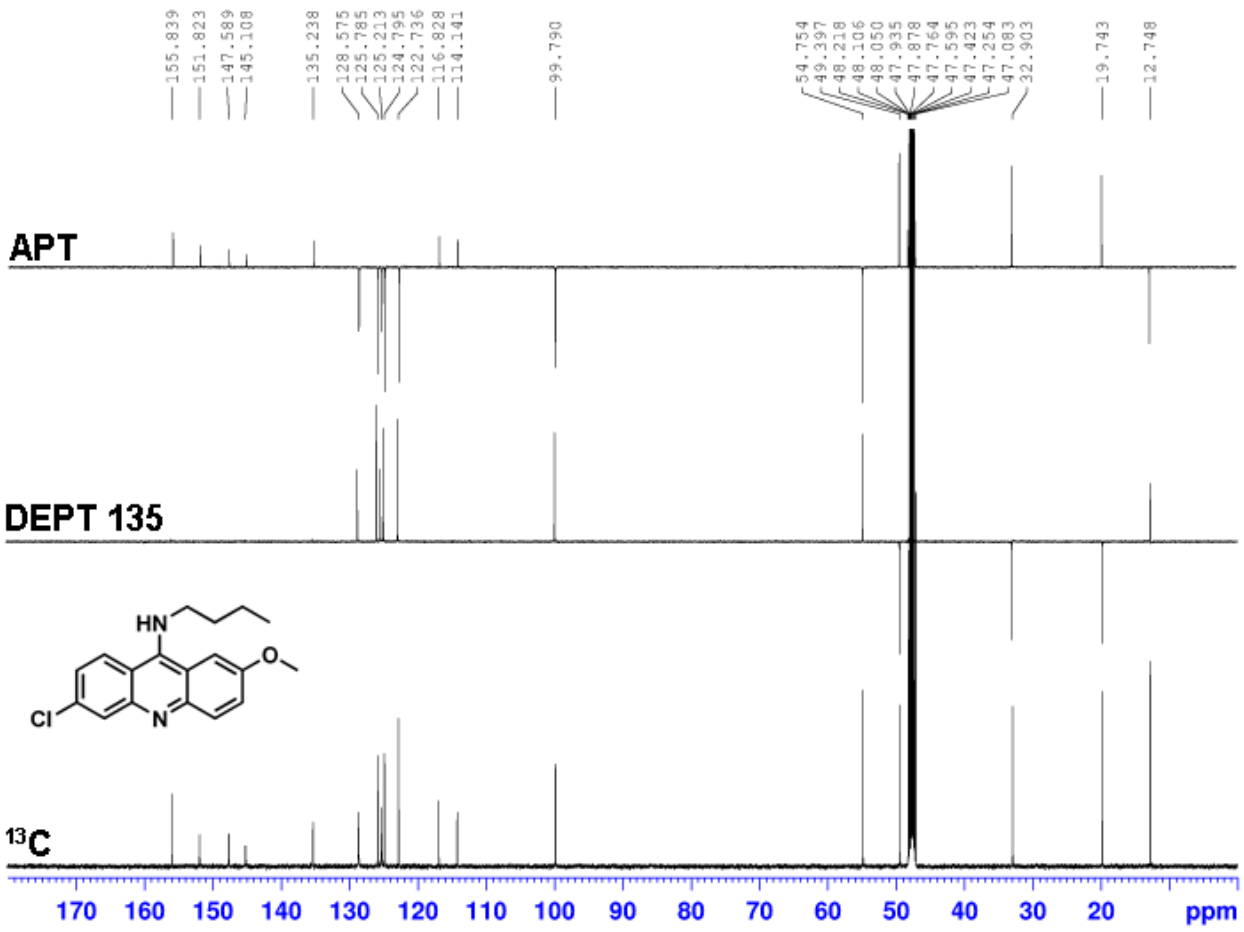

Figure S38: 125 MHz ^{13}C, DEPT-135 and APT spectra of **5** in MeOD at room temperature.

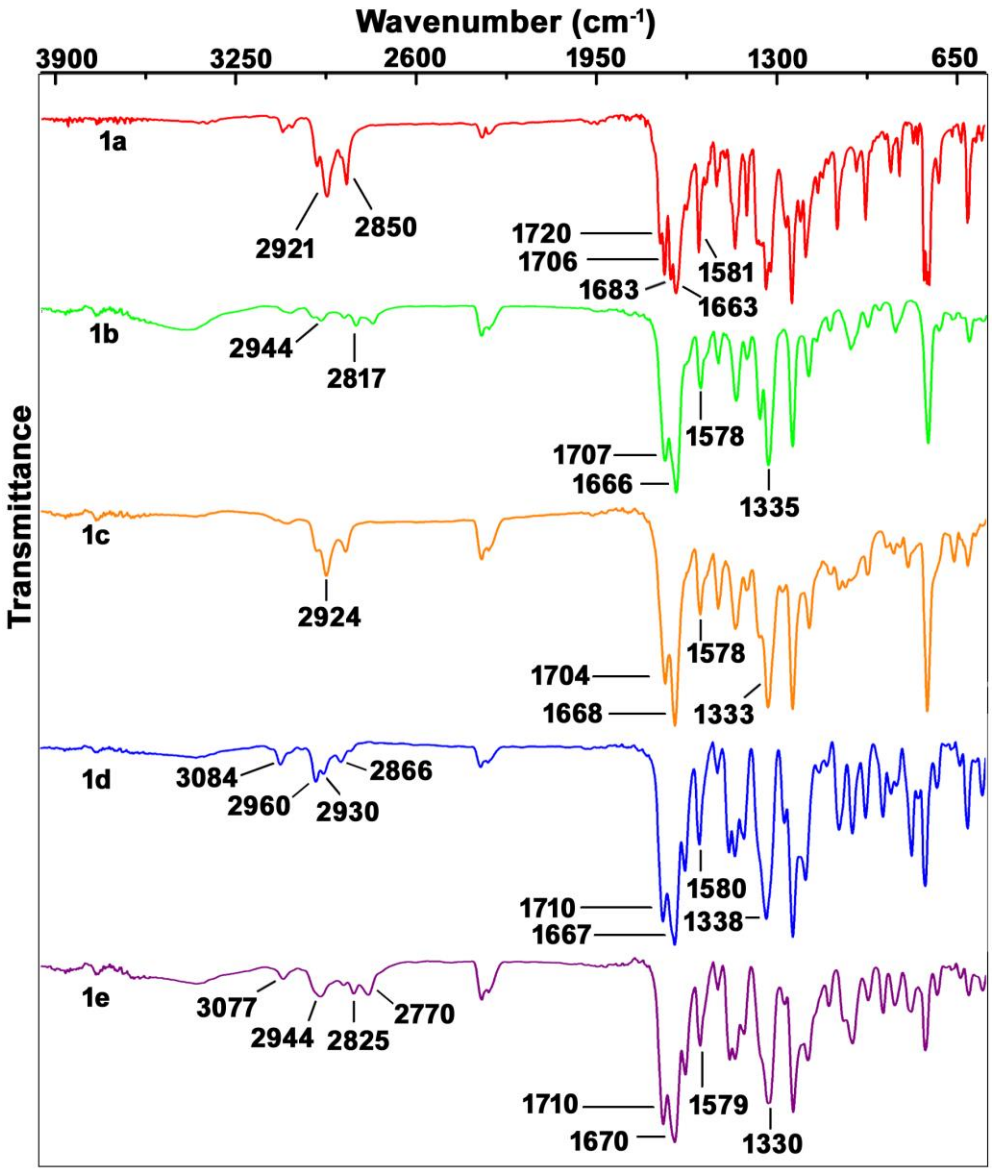

Figure S39: FT-IR spectra of **1a-e**.

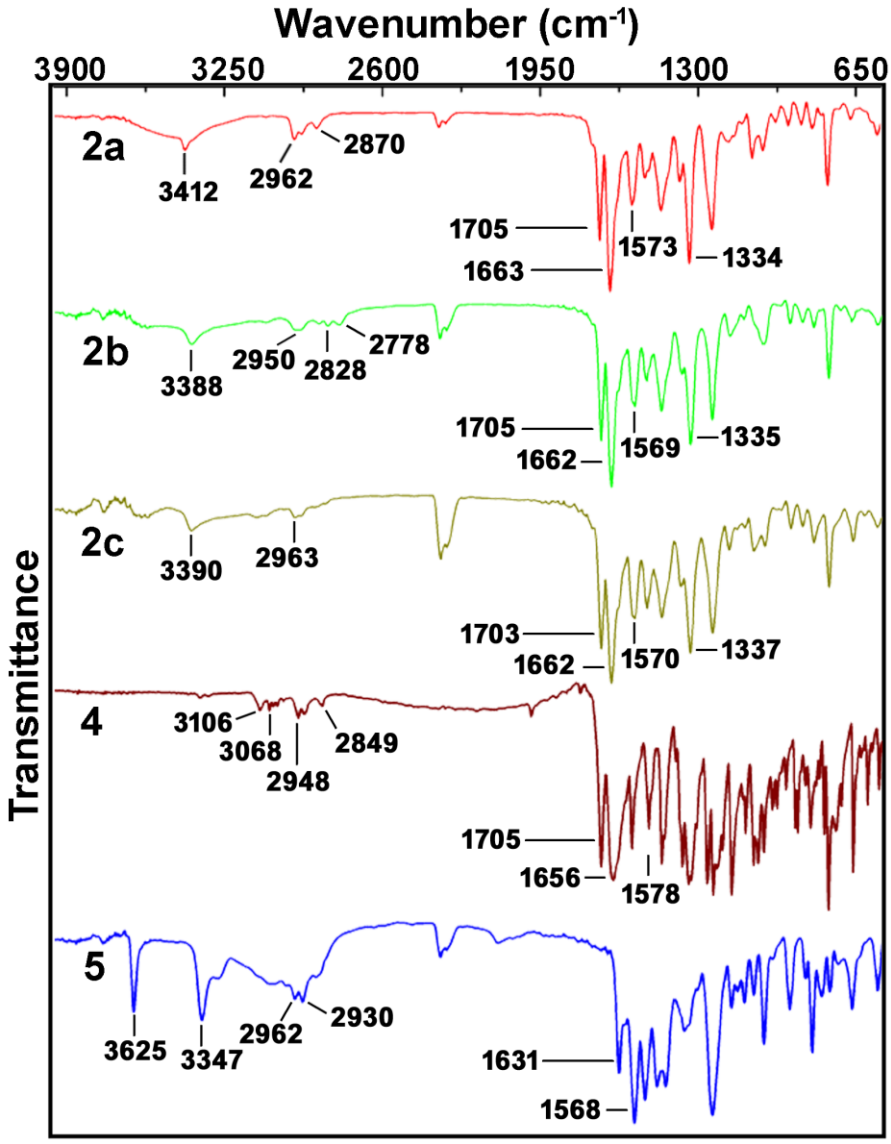

Figure S40: FT-IR spectra of **2a-c**, **4**, and **5**.

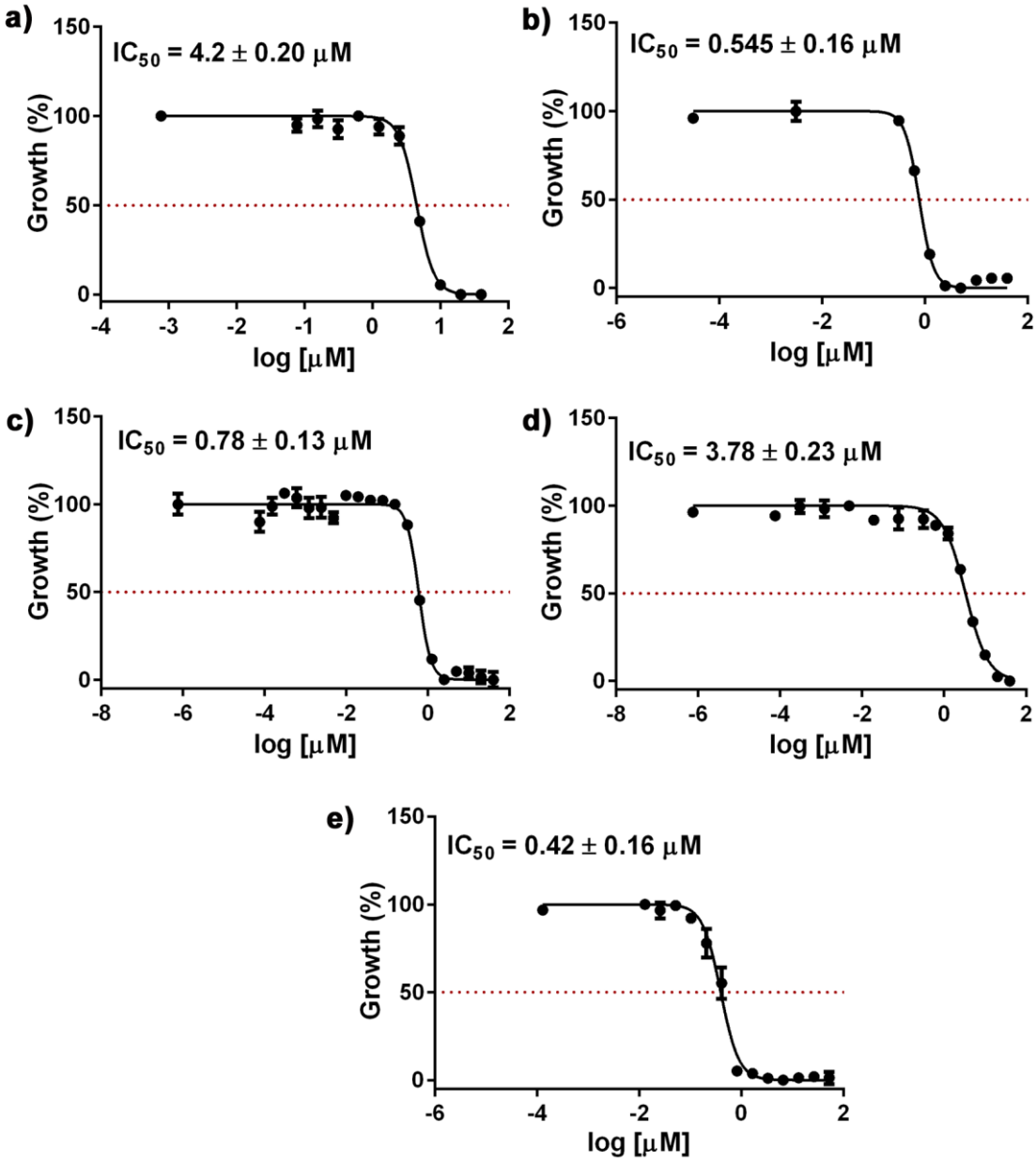

Figure S41: Effects of compounds **1a** (a), **1b** (b), **1c** (c), **1d** (d) and **1e** (e) on *in vitro* growth of *Plasmodium falciparum* 3D7 parasites. IC_{50}s were determined using SYBR Green I assay. Data represents mean ± SEM form two independent experiments with duplicates.

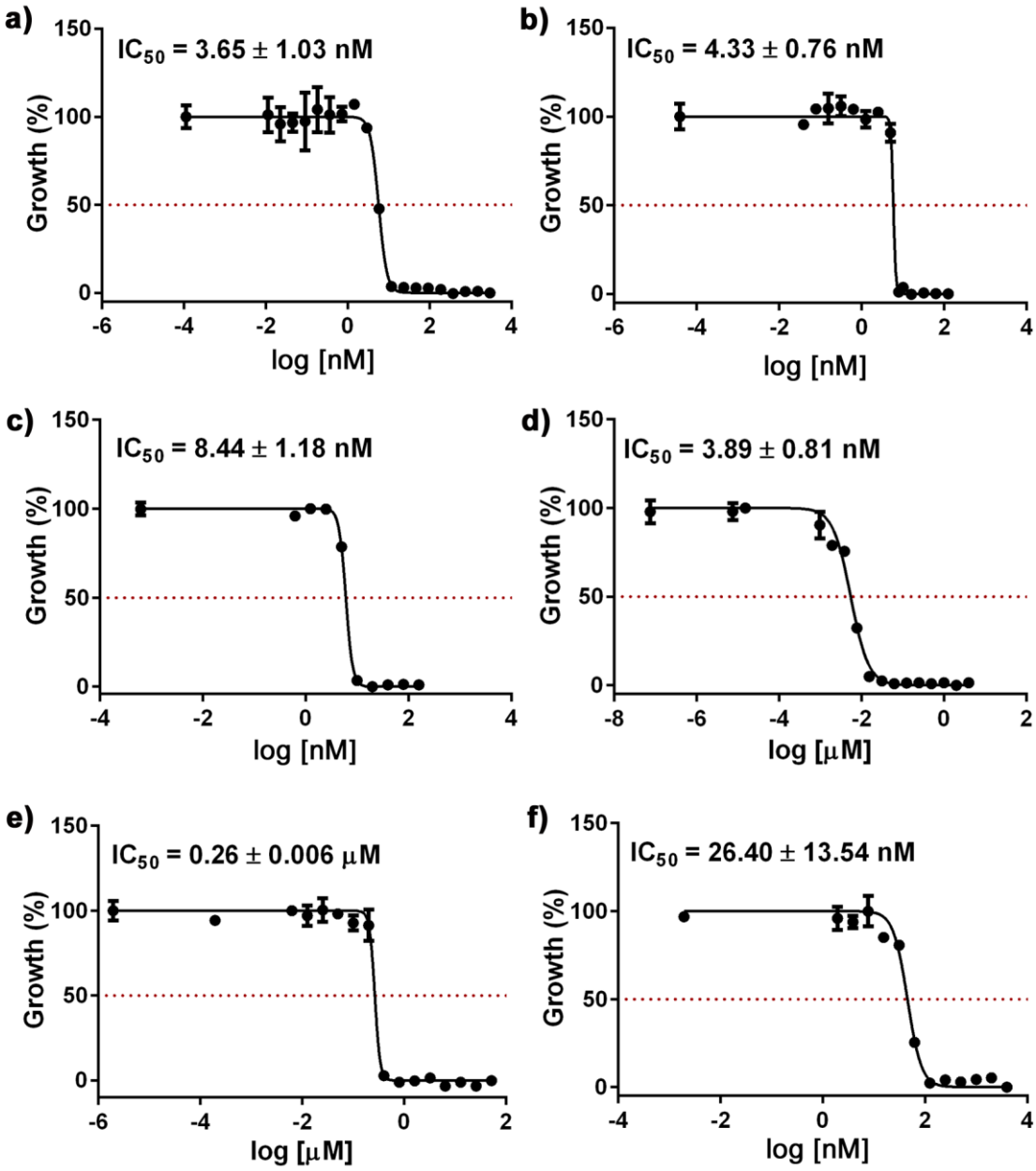

Figure S42: Efefcts of compounds **2a** (a), **2b** (b), **2c** (c), **3** (d), **4** (e) and **5** (f) on *in vitro* growth of *Plasmodium falciparum* 3D7 parasites. IC_{50}s were determined using SYBR Green I assay. Data represents mean ± SEM form two independent experiments with duplicates.

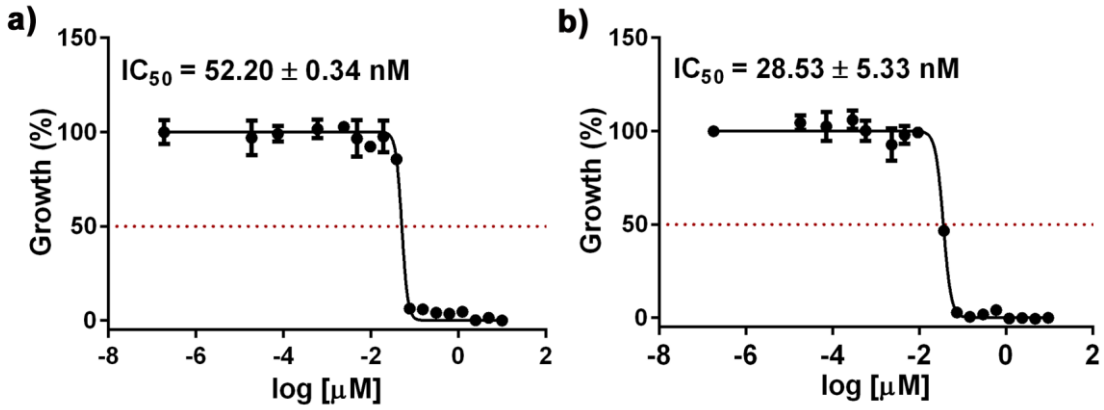

Figure S43: Efefcts of compounds **2a** (a) and **2b** (b) on *in vitro* growth of *Plasmodium falciparum* W2 parasites. IC_{50}s were determined using SYBR Green I assay. Data represents mean ± SEM form two independent experiments with duplicates.

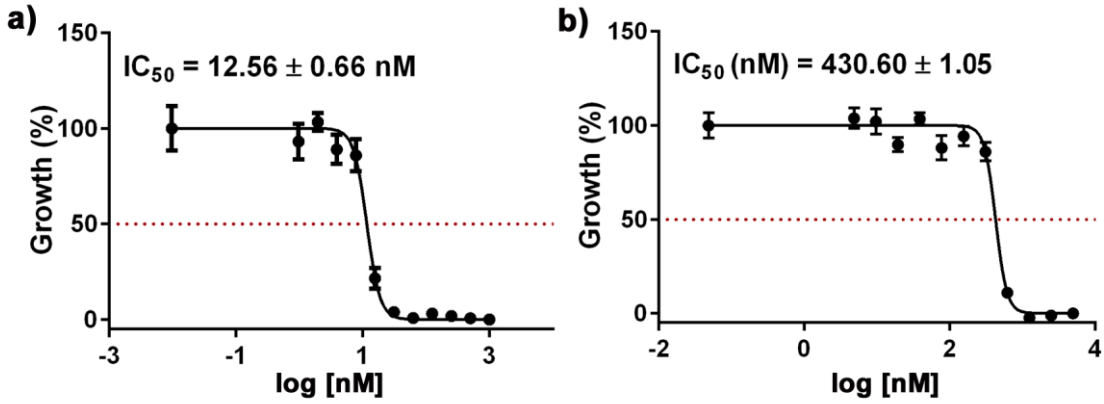

Figure S44: Efefcts of CQ on *in vitro* growths of *Plasmodium falciparum* 3D7 (a) and W2 (b) parasites. IC_{50}s were determined using SYBR Green I assay. Data represents mean ± SEM form two independent experiments with duplicates.

References

1. Van Meerloo, J.; Kaspers, G. J.; Cloos, J., Cell sensitivity assays: the MTT assay. *Methods Mol. Biol.* **2011**, *731*, 237-245.
2. Sharma, N.; Mohanakrishnan, D.; Shard, A.; Sharma, A.; Saima; Sinha, A. K.; Sahal, D. Stilbene-chalcone hybrids: design, synthesis, and evaluation as a new class of antimalarial scaffolds that trigger cell death through stage specific apoptosis. *J. Med. Chem.* **2012**, *55*, 297-311.